SALT TRANSPORT IN SOIL PROFILES WITH APPLICATION TO IRRIGATION RETURN FLOW

The Dissolution and Transport of Gypsum in Soils

by

T. K. Glas and D. B. McWhorter

January 1976

Completion Report Series
No. 71

SALT TRANSPORT IN SOIL PROFILES WITH APPLICATION TO IRRIGATION RETURN FLOW

The Dissolution and Transport of Gypsum in Soils

Completion Report
OWRT Project No. A-017-COLO

T. K. Glas and D. B. McWhorter

Department of Agronomy and Department
of Agricultural Engineering,
Colorado State University

Submitted to

Office of Water Research and Technology

January, 1976

The work upon which this report is based was supported (in part) by funds provided by the U. S. Department of the Interior, Office of Water Research and Technology, as authorized by the Water Resources Research Act of 1964 and pursuant to Grant Agreement Nos. 14-31-0001-3806, 14-31-0001-4006, and 14-31-0001-5006.

Colorado Water Resources Research Institute
Colorado State University
Fort Collins, Colorado 80523

Norman A. Evans, Director

ABSTRACT

SALT TRANSPORT IN SOIL PROFILES WITH APPLICATION TO IRRIGATION RETURN FLOW

Experimental information on the dissolution of gypsum and the subsequent transport of the dissolved species in a soil-water system was obtained by measuring the calcium concentration in the solution phase as a function of time at different positions in columns filled with a soil-gypsum mixture that were leached with distilled water. These gypsum leaching experiments were performed with two different soils for a range of flow rates of the solution phase, solution contents and particle sizes of the gypsum material.

The measured concentration-time curves were compared with results from two models, the first based on equilibrium chemical principles and the mixing cell concept and a second based on the one-dimensional convection-dispersion equation combined with a first-order kinetic rate equation describing the gypsum dissolution process. The formulation of the rate equation was based on the hypothesis that the rate of dissolution was proportional to the product of the saturation deficit and a function of the mass of gypsum present in the system.

The equations in the kinetic model were solved numerically and a graphical and an optimization procedure were used to determine those values of the kinetic parameters for which the best possible agreement was obtained between the measured concentration-time curves and curves calculated from the kinetic model.

It was concluded from the comparison between the experimental data, the mixing cell model and the kinetic model that the dissolution reaction of the gypsum was time dependent and was not controlled by the solubility product relationship, as assumed in the mixing cell model. The

qualitative agreement between the kinetic model and the experimental results seems to support the hypothesis used in the formulation of the rate equation.

KEY WORDS: leaching, gypsum, salt transport, salt transport equation, numerical solution, dispersion-convection, source term, dissolution calcium sulfate, soil leaching, percolation, salt removal, water quality, dissolved solids, solubility

INTERPRETIVE SUMMARY

The leaching of salts from soils contributes to the salinity of irrigation return flow and hence to deterioration of water quality. In some instances gypsum is an important contributor to the salinity of the leachate. Three processes are involved in the movement of salts in soils: (1) bulk, convective flow of the solution phase, (2) diffusion and dispersion in response to concentration gradients, and (3) reactions such as precipitation, dissolution and adsorption. The leaching of solid phase gypsum from soil involves dissolution, followed by dispersion and convection of the dissolved gypsum. This study was conducted to evaluate two methods of describing or modeling the dissolution process. The first method, the mixing-cell model, uses concepts of equilibrium between the solid gypsum and that in solution. The second method, a kinetic model, does not assume equilibrium, but attempts to describe the rate of dissolution.

The results showed that under the conditions of the study, the dissolution process must be described kinetically, and that the equilibrium assumption was not valid. A kinetic model for the dissolution was proposed. A better understanding of the leaching process has been obtained as a result of this work.

COOPERATION AND ACKNOWLEDGEMENTS

In addition to the support from the Office of Water Research and Technology, U. S. Department of Interior, this research was also supported in part by the Agricultural Research Service, U. S. Department of Agriculture, and the Departments of Agronomy and Agricultural Engineering, Colorado State University.

Principle investigator for the project was Dr. D. B. McWhorter, Department of Agricultural Engineering. One graduate student, T. K. Glas, was supported by the project, and obtained the PhD degree in Agronomy. Other investigators were Drs. C. V. Cole and A. Klute, Agricultural Research Service and Agronomy Department, Colorado State University, and Dr. D. K. Sunada, Department of Civil Engineering, Colorado State University.

Invaluable assistance was also obtained from Dr. Paul Duchateau, Department of Mathematics, Colorado State University and from Dr. Dale F. Heermann, Agricultural Research Service, Fort Collins, Colorado.

PUBLICATIONS IN PREPARATION

A presentation of part of the results of this research was made by T. K. Glas at the Annual Meeting of the American Society of Agronomy, Knoxville, Tennessee, August 24-30, 1975.

A thesis entitled "The Dissolution and Transport of Gypsum in Soils" was prepared by T. K. Glas and has been accepted by the Graduate College, Colorado State University in partial fulfillment of the requirements for the PhD degree in Agronomy.

A paper is being prepared for submission to the Soil Science Society Proceedings.

OBJECTIVE

The objective of this research was to investigate the applicability of (1) the equilibrium-solubility product model and (2) a kinetic model for the dissolution and leaching of gypsum in soil.

TABLE OF CONTENTS

TABLE OF CONTENTS (Cont'd)

LIST OF FIGURES

LIST OF FIGURES (Cont'd)

LIST OF FIGURES (Cont'd)

LIST OF FIGURES (Cont'd)

LIST OF TABLES

CHAPTER I

INTRODUCTION

Gypsum ($CaSO_4 \cdot 2H_2O$) is found as extensive sedimentary deposits interbedded with limestones, sandstones or shales, as is the case in certain regions in Colorado. In these deposits gypsum occurs as coarsely crystalline material, as aggregate material with a parallel fibrous structure and as fine grained massive material (Berry and Mason, 1959). Gypsum is also used extensively in agriculture as a soil amendment because of its beneficial effects on plant growth and soil properties.

The effectiveness of gypsum as an amendment and fertilizer depends, among other factors, on the degree of subdivision of the material, which affects the rate of dissolution and subsequent transport through the soil in the solution phase. The transport of dissolved gypsum plays an important role in its agricultural use, from the fertilizer and amendment viewpoint. Three types of processes are involved in the transport of a chemical species in a porous medium: (a) bulk convective transport in the solution phase, (b) hydrodynamic dispersion and (c) chemical and physical reactions. The leaching of gypsum from a soil profile involves all of these. The reaction is the dissolution of the gypsum.

Two approaches have been used to describe dissolution and precipitation reactions of solid phase salts in porous media. The first approach is based on the assumption that the solid phase and the solution phase are in equilibrium at all times. Equilibrium chemical principles are used to describe the chemical reactions. In the second approach the dissolution-precipitation reactions are treated kinetically, with a specification of the time rate of dissolution. The primary objective of the present study was to investigate which of these two approaches

best describes the dissolution process in the leaching of gypsum from a soil, by a combined experimental and modeling approach.

CHAPTER II

THE TRANSPORT OF CHEMICALS IN SOILS

Modeling of Transport

Theories of transport in chromatographic colums have been considered for application to transport in soils (e.g., see Frissel and Poelstra, 1967 and Boast, 1973). There are various ways of classifying these theories, but for the present purpose we will consider two types, plate and rate theories (Van Deemter et al. 1956).

According to the plate theory approach the flow domain is assumed to consist of a finite number of plates or cells. Within each plate, variables such as concentrations are considered uniform. Plate theories of various levels of sophistication have been developed, but in the simpler ones the flow process is treated discontinuously, i.e., a volume element of solution is brought into a plate or cell, chemical equilibrium is attained, and a volume element of solution is then taken out of the cell. A model of this type was applied by Tanji et al. (1967) to the leaching of soil containing solid phase gypsum, exchangeable calcium and magnesium, and calcium and magnesium chloride in solution. Dutt et al. (1972) describe a model which combines a numerical solution of the one-dimensional water flow equation with a chemical model based on equilibrium principles which is capable of treating the processes of infiltration, redistribution and percolation of soil water, as well as cation exchange, and dissolution and precipitation of gypsum and calcium carbonate. The modeling of such a complex system becomes feasible because of the assumption of chemical equilibrium. The principle drawbacks of the model are the perhaps questionable validity of the equilibrium assumption under certain conditions, the discontinuous treatment of the flow process,

and the more-or-less accidental simulation of the dispersion process through a built-in numerical dispersion (Tanji et al. 1967).

Rate models are based on the balance of mass, and flux concepts, in combination with some kind of kinetic expression for the reaction. At the macroscopic level (Bear, 1972; Raats and Klute, 1968) the one-dimensional form of the balance of mass for a component of the solution phase is:

$$\frac{\partial \rho_i}{\partial t} = - \frac{\partial F_i}{\partial z} + G_i \quad , \tag{1}$$

in which ρ_i is the mass of component i per unit volume of porous medium, F_i is the mass flux (density) of the component, G_i is the rate of production of the component by reactions per unit time and per unit volume of porous medium. The mass flux is composed of a diffusion-dispersion flux, J_i , and a convective flux, $c_i Q$. The diffusion flux is usually assumed to be proportional to the solution phase concentration gradient so that:

$$F_i = - D_i \theta \frac{\partial c_i}{\partial z} + c_i Q \tag{2}$$

where c_i is the mass of i per unit volume of solution phase, and Q is the volumetric solution phase flux. The hydrodynamic dispersion coefficient D_i is assumed to include the effects of hydraulic dispersion and molecular diffusion (Bear, 1972). Combining Eqs. (1) and (2) and using $\rho_i = c_i \theta$ the resulting equation of transport for the component becomes:

$$\frac{\partial (c_i \theta)}{\partial t} = \frac{\partial}{\partial z} \left(D_i \theta \frac{\partial c_i}{\partial z} \right) - \frac{\partial (c_i Q)}{\partial z} + G_i \quad . \tag{3}$$

The dispersion coefficient D_i depends on the properties of the porous medium, the seepage velocity, U , and possibly the solution con-

content, θ . For example, Rose (1973) states that the data collected by Pfannkuch (1963) can be represented by:

$$\frac{D_i}{D_0} = 0.67 + \gamma P^n \qquad (4)$$

where D_0 is the molecular diffusivity of species i in "free space", $\gamma = 0.5$, $n = 1.2$ and P is the Peclet number given by:

$$P = Ud/D_0 \qquad (5)$$

where U is the seepage velocity and D is a characteristic microscopic length such as average pore size or grain size. The above is fairly representative of dispersion coefficient behavior in single grain media, such as sands, of rather uniform pore size. In aggregated media, the relation of D_i to P is more complex (Rose, 1973), but is grossly similar to that depicted in Eq. (4). The effect of the solution content on the dispersion coefficient has not been extensively studied (e.g., see Nielsen and Biggar, 1961 and 1962; Gupta et al., 1973a, 1973b) and the results are not too conclusive. In this study the effect of θ on D_i will be ignored.

The dispersion coefficient is usually measured by analysis of breakthrough curves, i.e., the concentration-time curve for the effluent from a finite column of porous medium, which has been subjected to a displacement of one solution by another. Either the initial solution or the displacing solution may be water. Experimental conditions are normally arranged so that θ and Q are constant in the column of porous medium and G_i is zero. Under these conditions D_i is constant and Eq. (3) reduces to:

$$\frac{\partial c_i}{\partial t} = D_i \frac{\partial^2 c_i}{\partial z^2} - U_i \frac{\partial c_i}{\partial z} \qquad . \qquad (6)$$

Analytic solutions to (6) subject to various boundary conditions are available (Brenner, 1962; Ogata and Banks, 1961; Gerson and Nir, 1969). To determine the dispersion coefficient the breakthrough curve is measured and matched to the analytic solution of (6). Rose and Passioura (1971) give a convenient procedure for this. If there is no interaction of any kind between the component and the porous medium the seepage velocity may be calculated from the Darcy velocity and the solution content. In the case of an anionic species such as Cl^- the phenomenon of anion exclusion may be present to a significant degree, especially in media with appreciable clay content. Part of the solution phase volume is not accessible to the anion because it is to a greater or less degree repelled from the vicinity of the negatively charged surfaces of the clay. One of the results of this is that the effective seepage velocity for the anion is higher than it would appear to be from the Darcy velocity and the solution content (Smith, 1972). Looked at another way the volume of pores occupied by the anion is less than the total liquid filled pore space. If anion exclusion is present to a significant degree both D_i and U must be determined by the breakthrough curve matching procedure. Usually this process involves an optimization procedure to get the best trial-and error fit between the experimental data and the analytic solution to the transport equation.

If the chemical species being transported by convection and dispersion is also involved in a reaction and is thereby immobilized, the source function in Eq. (3) can be treated as follows:
The mass balance for the adsorbed immobile species is:

$$\frac{\partial \rho_a}{\partial t} = G_a \quad . \tag{7}$$

Assuming that the adsorption reaction is the only one in which the species is involved so that $G_a + G_i = 0$ we have then:

$$\frac{\partial \rho_a}{\partial t} = -G_i \quad . \tag{8}$$

Usually the concentration of adsorbed material is expressed as the mass of adsorbed species per unit mass of soil, N_a . Using the relation

$$\rho_a = \beta N_a \tag{9}$$

where β is the bulk density, which we shall consider as constant, Eq. (3) becomes:

$$\frac{\partial (c_i \theta)}{\partial t} = \frac{\partial}{\partial z} \left(D_i \theta \frac{\partial c_i}{\partial z} \right) - \frac{\partial (Q c_i)}{\partial z} - \frac{\beta \partial N_a}{\partial t} \tag{10}$$

in which $\partial N_a / \partial t$ is the time rate of change of the adsorbed phase concentration. If equilibrium between the adsorbed species and the free species is assumed, an isotherm, which expresses the equilibrium relation between c_i and N_a , can be used to evaluate the last right hand term in (10). An isotherm is of the form

$$N_a = f(c_i) \tag{11}$$

and if the function f is continuous and has a derivative then:

$$\frac{\partial N_a}{\partial t} = \frac{df}{dc_i} \frac{\partial c_i}{\partial t} = f' \frac{\partial c_i}{\partial t} \tag{12}$$

where f' is the slope of the isotherm. In general, f' will be a function of c_i . Substitution of (12) into (10) gives:

$$\frac{\partial (c_i \theta)}{\partial t} = \frac{\partial}{\partial z} \left(D_i \theta \frac{\partial c_i}{\partial z} \right) - \frac{\partial (Q c_i)}{\partial z} - \beta f' \frac{\partial c_i}{\partial t} \tag{13}$$

as the transport equation applicable to the dispersion-convection and reaction of a species that is immobilized by adsorption when equilibrium between the adsorbed and free states is assumed to exist. The isotherm

can possibly be measured independently of the system whose behavior is to be predicted by a solution of Eq. (13). If so, this is a major advantage resulting from the assumption of equilibrium.

If a solid phase salt is in equilibrium with its dissolved components in a solution that does not contain any other species, the concentrations of the components in solution are determined by the solubility product relationship, and will be equal to the saturated concentrations as long as any solid phase is present. Mathematically this can be written:

$$c = c_S \qquad \text{for} \quad N>0$$

$$c < c_S \qquad \text{for} \quad N=0$$

where c_S is the concentration of the dissolved components in equilibrium with the solid phase. For such a relation between N and c the derivative f' in Eq. (12) does not exist. Consequently the isotherm concept as it is used in adsorption reactions cannot be applied to dissolution processes and Eq. (13) or a simplification of it cannot be used.

An alternate approach to the treatment of the source function involves a specification of the rate of production of the dissolved species G_i. The rate of adsorption, which is the negative of the rate of production of the mobile species, is in general a function of N_a and c_i. Kinetic expressions for G_i can be of many forms, depending on the nature of the reaction. Chemical and physical reactions can be of zero order, first order, a higher order or a fractional order. The rate parameters may be constants or functions of one or more system properties. The reaction may be reversible or irreversible, and there may be multiple coupled reactions occurring simultaneously. In practice only the simpler kinetic expressions have been used (Frissel and Poelstra, 1967; Boast, (1973).

Equilibrium Chemistry of Gypsum

The dissolution-precipitation reaction for gypsum can be written as:

$$CaSO_4 \cdot 2H_2O_{solid} \rightleftarrows Ca^{2+} + SO_4^{2-} + 2H_2O \qquad (14)$$

The solubility product for gypsum is defined as:

$$K_{sp} = (Ca^{2+})(SO_4^{2-}) \qquad (15)$$

where the parentheses denote ionic activities. The activities of the solid phase and the water are set equal to unity by convention. As noted by Nakayama (1971) activities cannot usually be measured directly, but have to be calculated from measured concentrations. The calculation involves an estimate of the activity coefficients which are essentially factors correcting for the non-ideal behavior of electrolyte solutions due to electrostatic interactions between ions. In dilute solutions activity coefficients can be calculated using the concept of ionic strength and the Debye-Hückel equation (e.g. see Adams, 1972). An appreciable fraction of the cations and anions of certain electrolytes in solution behave as if un-ionized and are called ion-pairs. The association of free ions to form ion-pairs is expressed as a dissociation reaction, which for the ion-pair $CaSO_4^0$ is:

$$CaSO_4^0 \rightleftarrows Ca^{2+} + SO_4^{2-} \quad . \qquad (16)$$

The equilibrium dissociation constant for this reaction is:

$$K_D = \frac{(Ca^{2+})(SO_4^{2-})}{(CaSO_4^0)} \quad . \qquad (17)$$

The activity coefficient of the ion-pair is generally assumed to be unity.

General principles applying to ion-pair formation of common soil solution cations and anions are given by Adams (1972). Considerable research has been devoted to the determination of the solubility product of gypsum (Rance and Davey, 1968; Bennet and Adams, 1972) and the solubility of gypsum in water and in solutions containing different salts at varying concentrations (Longenecker and Lyerly, 1959; Tanji, 1969). Values of the solubility product[1] reported in the literature range from 2.4×10^{-5} to 4.24×10^{-5} at 25°C, with perhaps the most commonly used value about 2.5×10^{-5}. Measured solubilities of gypsum in water range from 30.2 to 30.6 meq/l. The solubility increases in the presence of non-common ions due to the ionic strength effect on the activity coefficients, and decreases in the presence of common ions.

The most commonly used value for the dissociation constant of $CaSO_4^0$ is 4.9×10^{-3}. In a solution containing only solid phase gypsum and its dissolved components the concentration of the ion-pair is constant and can be calculated from:

$$(CaSO_4^0) = \frac{K_{sp}}{K_D} \qquad (18)$$

which is obtained by combining Eqs. (15) and (17). For $K_{sp} = 2.5 \times 10^{-5}$ the concentration of the ion-pair is 5.1 mmol/l or about 35 percent of the total calcium concentration.

Kinetics of Dissolution

From a microscopic viewpoint the dissolution of a solid phase particle is heterogeneous since it takes place at the surface of the dissolving particle. In general, heterogeneous reactions involve three

---

[1]Activities and concentrations are usually expressed in moles per liter.

steps: the transfer of reactants to the reaction surface, the reaction itself, and the transfer of the products away from the reaction surface. In the case of the dissolution of gypsum particles only the last two of these are involved. The rate of the overall reaction will be determined by the slowest step. If the transfer of products or reactants is the rate determining step, the reaction is said to be diffusion or transport controlled. In the opposite case, the chemical reaction is the slowest step and the rate is determined by chemical kinetics.

According to Levich (1962) the dissolution of most solids in liquids is diffusion controlled. Weyl (1958) showed experimentally that this is the case for the dissolution of limestone particles. Barton and Wilde (1971), using a rotating disc method, determined that the dissolution of gypsum was transport controlled, while that of anhydrite ($CaSO_4$) was intermediate between chemical and transport controlled.

An empirical relation for dissolution of solids in liquids based on extensive experimental data was given by Shchukarev (1891) as:

$$\frac{dm}{dt} = KA(c_S - c) \tag{19}$$

where m is the amount of solid phase material per unit volume of solution at time t, A is the surface area of the dissolving material per unit volume of solution, c_S is the concentration in a solution saturated with the dissolving material, c is the concentration in solution at a given distance from the particle and K is a proportionality constant $(L^{-2}T^{-1})$.

Further studies, especially by Nernst (1904), showed that K was proportional to D_0 the diffusion coefficient of the dissolved substance in the solvent, and led to the following expression for the dissolution

rate:

$$\frac{dm}{dt} = \frac{D_0 A}{\delta} (c_s - c) \qquad (20)$$

where δ is a constant designating the thickness of the region through which the solute diffuses. Equation (20) is an expression for the diffussion flux in a static liquid layer of thickness δ, with a concentration difference across it equal to $c_s - c$. It is assumed that the liquid is always saturated with the solute immediately adjacent to the surface of the particle. In a case where mass transfer takes place due to convective motion of the solution phase, Nernst assumed that there is a thin layer of static liquid of thickness δ next to the particle. The theory has been criticized on several grounds. Equation (20) does not permit dm/dt to be calculated *a priori* because δ is not known independently. Experimental measurements have shown that liquid motion may be observed at distances 1/10 to 1/100 of that assumed by Nernst. It has also been found that δ apparently depends in some way on D_0. Levich concludes that the Nernst theory is basically incorrect and only has value as an empirical relation.

Levich develops a more rigorous treatment of the dissolution of a particle based on the convection-diffusion equation. In this theory a diffusion boundary layer concept is developed, but it differs fundamentally from the static boundary layer concept in Nernsts' theory, in that it accounts for the motion of the liquid inside the layer and the mass transfer induced by it. However, Levich showed that the diffusional flux through the boundary layer can be approximated by an expression

similar to equation (20) where δ is now a known function of the fluid properties, the fluid velocity, and D_0.

By combining the convective and diffusive fluxes an expression for the time rate of decrease of the mass of a single particle can be derived (Bird et al. 1960). The resulting equation is similar to Eq. (19), with the parameter K designated as a mass transfer coefficient. Ranz and Marshall (1952), in a study of mass transfer from liquid drops, obtained an expression for the mass transfer coefficient in terms of the radius of the drop, the fluid properties, the fluid velocity, and the diffusion coefficient. Using these results Millington and Powrie (1968) calculated the time rate of dissolution of a single fertilizer granule. They concluded that the rate of dissolution was diffusion controlled and that the magnitude of the flow velocities of the soil solution encountered under field conditions was too small to have any significant effect on the dissolution process.

A somewhat different approach to a theory of the dissolution of a particle is embodied in the equal reduction hypothesis which was advanced by Bear and Allen (1932) in a study of the effect of particle size on the rate of dissolution of limestone. In this hypothesis the rate of dissolution is assumed proportional to the surface area and the rate of reduction of the diameter of the particles is considered to be independent of the diameter. Bear and Allen concluded that the hypothesis was approximately valid for particles less than 0.1 mm in diameter. Elphick (1955) used the equal reduction hypothesis in a study of limestone dissolution and also considered that predictions based on the hypothesis were successful. Swartzendruber and Barber (1965) derived a dissolution equation using the equal reduction hypothesis based on

spherical particles of uniform size, density and composition. In this case, since the mass of a particle is proportional to the cube of the particle radius we have:

$$\frac{dm}{dt} = c_1 \frac{dr^3}{dt} = c_1 r^2 \frac{dr}{dt}$$

where c_1 is a constant. According to the equal reduction hypothesis, dr/dt is independent of r and is constant. At any time t the surface area of a particle is proportional to r^2 so that:

$$\frac{dm}{dt} = c_2 f^2 = KA \qquad (21)$$

where K is a negative constant. After examination of Elphick's data, Swartzendruber and Barber concluded that for particles less than 0.5 mm diameter the assumption of equal reduction did not hold, and that the rate of dissolution was not proportional to the surface area. They proposed an alternative rate equation of the form of Eq. (20) but did not test its experimental validity.

The literature reviewed above clearly indicates that the particle size of the gypsum is an important factor in determining its rate of dissolution. However, there do not seem to have been any attempts to incorporate the dissolution process into the transport equation for prediction purposes.

CHAPTER III

MATERIALS, EQUIPMENT AND METHODS

One of the objectives of this study was to obtain experimental information on the dissolution of solid phase gypsum in a dynamic soil-water system. In order to accomplish this objective and to facilitate the testing of proposed dissolution models, an idealized experimental system, as compared to a field situation, was devised. Known amounts of gypsum with varying particle sizes were mixed with two different soils. The mixtures were packed in columns. The initial solution phase was saturated with gypsum. The gypsum was leached from the column with water, and the solution phase was sampled at regular times and at several elevations.

Two soil materials were used in the columns: one a sand, the other a clay. Tables 1 and 2 show the results of various physical and chemical analyses of the soil materials. The sand was from the surface horizons (0-30 cm) of a soil mapped as Blakeland sand in Washington County, Colorado. The clay was from the 20-35 cm depth of a Weld clay from near Greeley, Colorado.

The exchange complex of the clay was saturated with calcium by leaching with 5N $CaCl_2$ until Mg^{2+} could not be detected in the effluent by the EDTA titration method (Richards, 1954). The excess salt was then removed by leaching with distilled water until no precipitate was formed upon addition of $AgNO_3$ to the effluent. The soil was then redried, crushed and passed through a 2 mm sieve. More than 95 percent of the exchange complex was occupied by Ca^{2+} after this process.

The sand contained some solid phase carbonates. In part of the sand, this was removed by treatment with 3N HCl , followed by leaching with water until the pH of the leachate equaled that of the water.

Table 1. Some physical properties of the soils used.

Soil:	Sand	Clay
Sieving analysis		
0.05 - 0.125 mm	8%	
0.125 - 0.25 mm	31%	
0.25 - 0.5 mm	53%	
0.5 - 1.0 mm	5%	
1.0 - 2.0 mm	1%	
Particle size distribution		
Sand (0.05 - 2 mm)	98%	21%
Silt		33%
Clay		46%
Particle density P_d (g/cm^3)	2.65	2.69
Sat. hydraulic cond. (cm/hr)	1.28	0.24

Table 2. Some chemical properties of the soils used.

Soil:	Sand	Clay
Cation exchange capacity (meq/100 g)	5.0	25.7
Exchange complex composition		
Ca	88%	55%
Mg	7%	41%
Na	1%	1%
K	4%	3%
Saturated paste		
Water content (% weight)	21.3	60.9
pH	8.06	7.65
EC (mmho/cm)	0.31	0.24
Ca (meq/l)	2.6	1.2
Mg (meq/l)	0.3	1.0
Na (meq/l)	0.6	0.3
K (meq/l)	0.5	0.1
Carbonate content (% weight)	0.1	nil

Water content-pressure head drainage relationships (see Fig. 1) were determined for both soils using weighable cells similar to those used by Reginato and Van Bavel (1962).

The agricultural gypsum used in this study was obtained from a commercial plant in Salida, Colorado. The material was separated into the following size ranges: 63 , 63-125 , 125-250 , 250-500 , 500-1000 and 1000-2000 . In a few experiments, reagent grade powdered gypsum was used. This material was either mixed directly with the soil, or applied by evaporation of a saturated gypsum solution ponded on a thin layer of soil. The dried soil-gypsum mixture was crushed and passed through a 2 mm sieve.

The purity of the gypsum material was measured by shaking 0.5 g of each of the finely ground size ranges with 250 ml of distilled water for time periods varying from 167 to 592 hours. The dissolution rate of each size fraction was determined by shaking 0.5 g samples (unground) in 250 ml water. Solution samples (2 ml) were removed at 1, 3, 6, 12, 23, 36, 72, 119 and 167 hours. Calcium analyses were made with a Perkin-Elmer atomic absorption spectrophotometer (AA). Some samples were analyzed for sulfate by a turbidimetric procedure as a $BaSO_4$ precipitate suspended in a gum arabic solution. This procedure was a slight modification of the method described by Massoumi and Cornfield (1963). The solubility of the various size fractions of the gypsum material was measured by shaking an excess (1.25 g) of the finely ground gypsum with distilled water (250 ml) and determining the calcium concentration in the solutions.

Some of the material in the 1-2 mm size range was separated by hand into three fractions. One fraction consisted of colorless particles

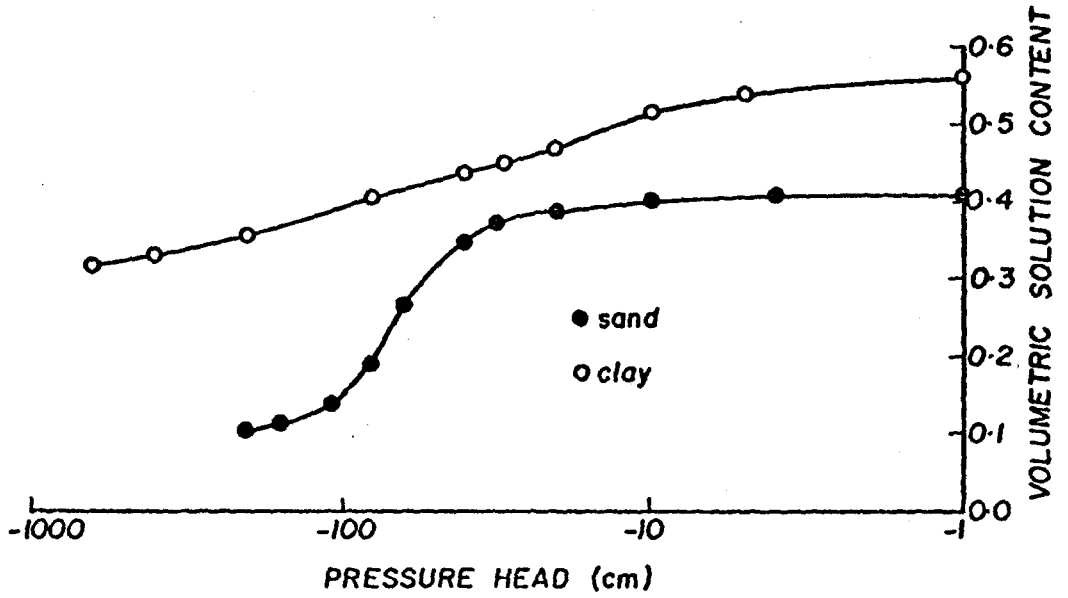

Fig. 1. Pressure head - solution content relationship for the sand and the clay soil.

with a crystalline appearance and white chalk-like pieces. A second fraction consisted of yellow mostly amorphous particles. The particles in the remaining fraction were dark gray or black with little crystalline structure. These fractions are referred to later as the white, yellow and black fractions. The purity of each fraction was determined as described above.

The carbonate content of each size fraction and the white, yellow and black fractions was measured using CO_2 evolution (Williams, 1948).

The experimental arrangement, which was used for conducting experiments under downward unsaturated flow of the solution phase, is shown in Fig. 2. A Lucite cylinder with an inside diameter of 15 cm and 33 cm long was used to contain the soil. Ceramic suction cups at two positions (10 and 20 cm from the bottom) were used to sample the solution phase. Duplicate tensiometers were installed at 5, 15 and 25 cm from the bottom of the column. A ceramic plate was used at the bottom of the column so that suction could be applied to the lower end of the soil column.

The air dry soil was mixed with the desired amount of one of the size ranges of gypsum, passed several times through a screen "particle distributor" of the type described by Wygal (1963) and then was placed in the column by passing it through the particle distributor. The column was filled to just above the position of the lower solution sampling tube. After tapping, the upper sampling tube was inserted and the column was filled until after settling a depth of about 30 cm of soil was obtained. The column was then wetted from the bottom with a saturated gypsum solution.

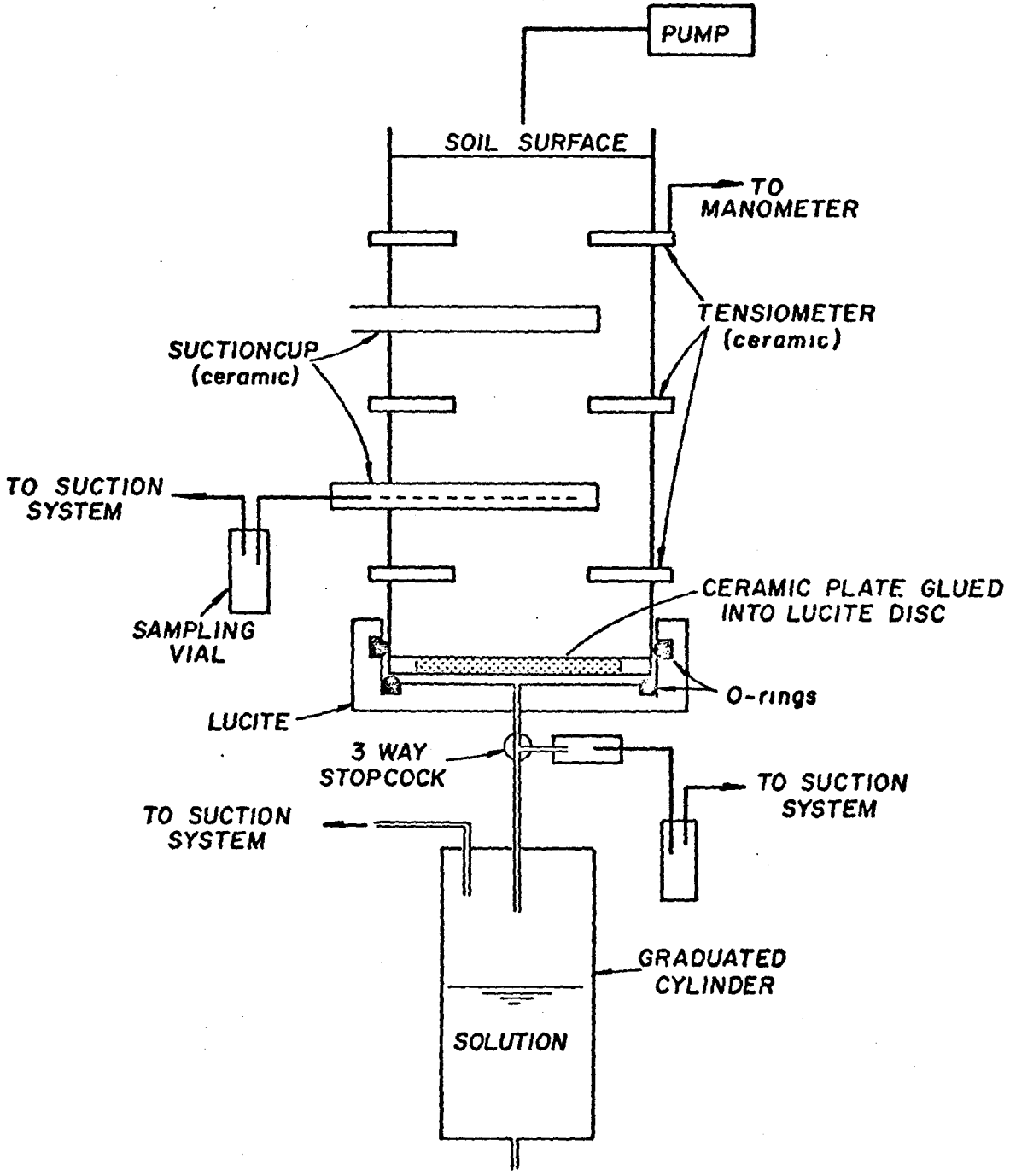

Fig. 2. Schematic overview of the experimental set-up used in the gypsum leaching studies.

After wetting the column a constant flow rate of the same solution was applied to the top of the column. By regulating the flow rate to less than that equivalent to the hydraulic conductivity of the saturated soil and by applying an appropriate suction at the bottom of the column, a condition of steady-state downward unsaturated flow with unit hydraulic gradient can be approached. Under this circumstance the pressure head and solution content would be constant. This constant-water content, constant-flux condition was desired in order to simplify the application of the models to the leaching system. Analysis shows that if the suction at the bottom is made larger than the ideal for unit gradient, the unit gradient condition will prevail throughout the column except for a limited region near the bottom.

When the solution phase came under suction the tensiometers were installed. Water manometers were used to display the hydraulic head (and pressure head) of the solution phase.

After the steady-state flow condition with a saturated gypsum solution was established, the initial solution was displaced by water at the same flow rate. The solution phase was sampled at three positions (at the outflow and 10 and 20 cm above the bottom of the column) at intervals of 4 to 6 hours. The solution samples were analyzed for calcium using the AA. In some samples sulfate was determined turbidimetrically as previously described. The leaching was continued until all or most of the solid phase gypsum was dissolved, and the calcium concentration approached zero. After termination of the flow the soil columns were separated into 2-3 cm long sections and the solution contents of the sections were determined.

The general procedures for experiments conducted under saturated flow conditions were similar to those described above. Most of the saturated flow experiments were conducted using Lucite cylinders with a diameter of 6.9 or 6.3 cm . No tensiometers were installed and a ceramic plate was not used at the bottom (outflow) end of the column. The columns were wetted with a saturated gypsum solution. Leaching was carried out by applying distilled water with a constant flow rate pump to the top of the column. The connecting tubing and reservoir between the pump and the column was closed, i.e., not open to the atmosphere. By this means a greater variation in flow rate was possible than would have been the case with ponded water open to the atmosphere at the top of the column.

To reduce the contribution by the ceramic suction cups used for solution sampling to the calcium in the extracted solution they were leached with 1N HCl until the Ca^{2+} concentration in the leachate was less than 0.1 meq/; (Grover and Lamborn, 1970). The excess Cl^- was removed by leaching with distilled water. It was assumed that any exchange capacity of the ceramic was saturated with Ca^{2+} ions during the initial wetting of the column with saturated gypsum solution.

Chloride breakthrough curves were measured and used to determine the dispersion coefficient. Most measurements were made under saturated conditions. The columns for these measurements were packed as described above and wetted with distilled water. The water was displaced with a KCl solution containing approximately 500 ppm Cl^- . A specific ion electrode was used to determine Cl^- in the effluent. After the water was displaced by the KCl solution the column was leached with distilled water to obtain a backward breakthrough curve. The cycle of forward and

backward breakthrough curves was repeated several times at different flow rates on a given soil column.

To investigate the uniformity of the initial soil gypsum mixture a sectioned Lucite column made from 10 rings with an i.d. of 5 cm and a height of 3 cm was filled with the mixture in a manner comparable to that used to fill the leaching columns. Samples of the mixture were taken from each 3 cm section, and the mass of gypsum in each was determined by dissolving (with shaking) the gypsum in water and determining the calcium concentration in the resulting solution.

CHAPTER IV

THEORETICAL ANALYSIS

In the leaching columns described for use in this study, at each point in the system (macroscopic viewpoint) there was a solution phase, a solid phase and possibly a gas phase. The solid phase consisted of the soil solids and gypsum, unless all the gypsum had been dissolved. The components of the solution phase were water, calcium ion, sulfate ion, and calcium sulfate ion-pair, unless all the dissolved gypsum had been displaced by the incoming water. The possible effects of sulfate adsorption by the soils, and exchange of adsorbed calcium ions by hydrogen ions were neglected.

Two models were applied to the gypsum leaching data, a mixing cell model and a kinetic model.

The Mixing-Cell Model

Equilibrium chemical principles are used in the mixing cell model, which is a simplified version of a model developed by Tanji et al. (1967). The continuous flow process is represented by a discontinuous sequence of flow followed by mixing and chemical equilibration.

The column is considered to consist of n segments of equal height $\Delta z = L/n$ where L is the length of the column. Each segment is identified by an index i, where $i=1,2,\ldots,n$. The time axis is divided into equal increments Δt which are indexed by j, where $j=1,2,\ldots$. At time j and position i the equilibrium concentration of a given species is denoted by $c_{i,j}$. A flow of solution at Darcy velocity q from layer $i-1$ to layer i, and from layer i to layer $i+1$, is assumed to occur in the time interval Δt . The concentration in layer i after the flow has occurred can be calculated from mass balance principles and is given

by:

$$c_{i,j+1} = c_{i,j} + \frac{\Delta t}{\Delta z}\frac{q}{\theta}(c_{i-1,j}-c_{i,j}) \quad . \qquad (21)$$

In developing Eq. (21) it is considered that no dispersion processes or chemical reactions occur during the flow, and that complete mixing in each cell is obtained. Due to the flow and mixing process the chemical equilibrium in each cell will be upset. Chemical reactions between the species will occur, which in the system being considered, are the possible dissolution of solid phase gypsum and formation of $CaSO_4^0$.

The changes in concentration due to chemical reactions can be calculated by an iterative procedure in which the values of $c_{i,j+1}$ are used as the first estimate, $c^1_{i,j+1}$, of the equilibrium concentrations. Successive estimates of the equilibrium concentrations, $c^k_{i,j+1}$, where K is an iteration index, k=1,2,...., are made by the following procedure: as long as solid phase gypsum is present in a layer, the concentration of $CaSO_4^0$ is constant at that point (se Eq. (18)). In this case the improved estimates of $[Ca]^{k+1}$ and $[SO_4]^{k+1}$, which are the estimates of the equilibrium concentrations of the calcium and sulfate ions in layer i and time j+1, are calculated from:

$$[Ca]^{k+1} = [Ca]^k + x \qquad (22)$$

$$[SO_4]^{k+1} = [SO_4]^k + x \qquad (23)$$

where x is the change in concentration of the ions due to dissolution of gypsum. Writing the solubility product for gypsum, Eq. (15), as:

$$K_{sp} = \gamma_{Ca}[Ca]^{k+1}\gamma_{SO_4}[SO_4]^{k+1}$$

and substituting (22) and (23) into this relation leads to:

$$x^2 + ([Ca]^k + [SO_4]^k)x + ([Ca]^k[SO_4]^k - \frac{K_{sp}}{\gamma_{Ca}\gamma_{SO_4}} = 0 \quad .(24)$$

In (24), γ_{Ca} and γ_{SO_4} are the activity coefficients of calcium and sulfate ion respectively and are estimated from the concentrations $c^k_{i,j+1}$. Equation (24) is a quadratic in x which can be solved for x and used in (22) and (23) to give $c^{k+1}_{i,j+1}$ for the calcium and sulfate ions.

When solid phase gypsum is no longer present, the concentration of $CaSO_4^0$ is no longer constant and Eq. (24) does not apply. In this case the dissociation of the ion-pair controls the concentrations of ionic calcium and sulfate. Improved estimates of the equilibrium concentrations are calculated from:

$$[Ca]^{k+1} = [Ca]^k - y \qquad (25)$$

$$[SO_4]^{k+1} = [SO_4]^k - y \qquad (26)$$

$$[CaSO_4^0]^{k+1} = [CaSO_4^0]^k + y \qquad (27)$$

where y is the change in concentrations due to ion-pair dissociation. Substitution of (25), (26) and (27) into Eq. (17) gives:

$$y^2 - ([Ca]^k + [SO_4]^k + \frac{K_D}{\gamma_{Ca}\gamma_{SO_4}})y + ([Ca]^k[SO_4]^k - \frac{K_D}{\gamma_{Ca}\gamma_{SO_4}}[CaSO_4^0]^k) = 0 \quad . \qquad (28)$$

Equation (28) can be solved for y which then can be used in (25), (26) and (27) to give the improved estimate of the equilibrium concentrations. The successive estimates of the equilibrium concentrations are then compared. If the difference between $c^{k+1}_{i,j+1}$ and $c^k_{i,j+1}$ for all the species is less than a small value ε, chemical equilibrium is considered

to be attained and the process advances to a new time step. If any of the differences are larger than ε, $c^{k}_{i,j+1}$ is replaced by $c^{k+1}_{i,j+1}$ and the iteration is repeated.

A flow chart of the above computation scheme is shown in Fig. 3.

The Kinetic Model

For the kinetic model it is assumed that Eq. (3) describes the transport of the dissolved gypsum. The mass balance of the immobile solid phase gypsum is given by Eq. (7). In the experimental system it is assumed that the dissolution of gypsum is the only reaction so that a pair of partial differential equations describes the transport and dissolution:

$$\frac{\partial(c\theta)}{\partial t} = \frac{\partial}{\partial z}\left(D\theta \frac{\partial c}{\partial z}\right) - \frac{\partial(Qc)}{\partial z} + G_g \tag{29}$$

$$\frac{\partial m}{\partial t} = -G_g \tag{30}$$

in which a model for the source function for dissolved gypsum, G_g, must be formulated. In these equations c is the concentration of dissolved gypsum in the solution phase and m is the mass of solid phase gypsum per unit volume of porous medium.

Several rate expressions representing the dissolution of a single solid phase particle into a liquid have been suggested in the literature. These expressions are only applicable on a microscopic scale in a porous medium, and a transition to the macroscopic level must be made before they can be used in Eqs. (29) and (30).

The solution immediately adjacent to the surface of the gypsum particles is assumed to be saturated, with concentration c_S. The concentration of dissolved gypsum in the solution away from the particle

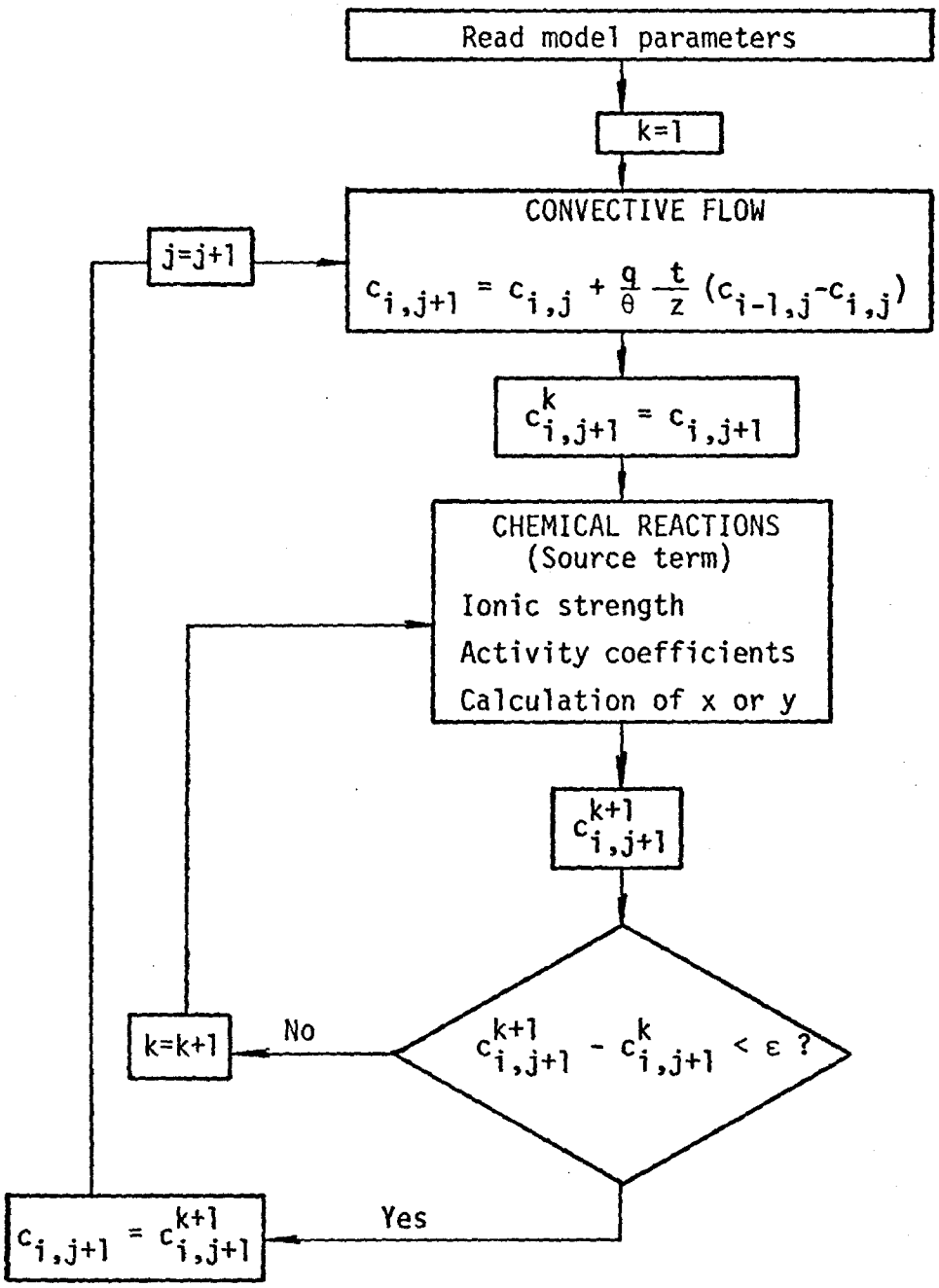

Fig. 3. Computation scheme in the mixing cell model.

will be denoted as $\bar{c}(z,t)$ where the bar indicates a variable defined on a microscopic scale. By combining expressions for the mass flux of the dissolving species resulting from the bulk motion of the fluid and from the diffusion superimposed on the bulk flow the following expression for the rate of dissolution of a gypsum particle can be derived (Bird et al., 1960):

$$\frac{\partial \bar{m}}{\partial t} = \bar{K}\bar{A}[\bar{c}(z,t) - c_s] \tag{31}$$

where $\bar{K}$ is a microscopic reaction rate parameter ($T^{-1}L^{-2}$) and $\bar{m}$ is the mass of the particle. Equation (31) was used by Millington and Powrie (1968) to describe the dissolution of a fertilizer granule. For particles with a common geometric shape it can be shown that

$$\bar{A} = f \left(\frac{\bar{m}}{\rho_p} \right)^{2/3} \tag{32}$$

where ρ_p is the density of the particle and f is a factor depending only on the particle shape. As the particle dissolves $\bar{m}$ changes with time. It is also possible and even likely that f will change with time. Thus $\bar{A}$ will be time dependent.

A transition from Eq. (31) at the microscopic level to a corresponding relation at the macroscopic level could conceptually be made by integrating Eq. (31) over a representative elementary volume (REV) of the porous medium in the manner described by Bear (1972) and by Raats and Klute (1968). The difficulty here is that one of the variables in the equation is the total surface area of the gypsum in the REV which cannot be calculated as a function of position and time. It does not seem possible to develop an expression for G_g beginning with Eq. (31). However, Eqs. (31) and (32) suggest that it might be possible to describe

the dissolution of gypsum on the macroscopic level by an expression in which the dissolution rate is proportional to the product of the saturation deficit $(c-c_S)$ and a dimensionless function of the mass of gypsum present per unit volume of porous medium, $F(m)$. Thus:

$$\frac{\partial m}{\partial t} = kF(m)\theta[c(z,t) - c_S] \tag{33}$$

where k is a reaction rate parameter. The function $F(m)$ should satisfy the following conditions:

(a) $F(0) = 0$, $F(m_i) = 1$

(b) $0 \leq F(m) \leq 1$; $0 \leq m \leq m_i$

(c) $dF/dm > 0$

(d) $F(m)$ is continuous for $0 \leq m \leq m_i$.

In the above m_i is the initial amount of solid phase gypsum present in the porous medium. Under the above conditions the dissolution rate is zero if all the gypsum is dissolved, and for a given saturation deficit $(c-c_S)$ the dissolution rate is larger if more solid phase gypsum is present. After investigating several functions satisfying the above conditions the following formulation for $F(m)$ was selected:

$$F(m) = \left(\frac{m}{m_i} \right)^{\alpha} \quad . \tag{34}$$

In Eq. (34), α is an empirical parameter that cannot be measured independently from the leaching data. Attempts to calculate α using theoretical considerations have been unsuccessful in part due to problems with the factor f in Eq. (32).

Using Eq. (34) in (33) and the result in turn in Eqs. (29) and (30) the transport equations become:

$$\frac{\partial(c\theta)}{\partial t} = \frac{\partial}{\partial z}\left(D\theta \frac{\partial c}{\partial z}\right) - \frac{\partial(Qc)}{\partial z} - K\theta \left(\frac{m}{m_i} \right)^{\alpha}(c-c_S) \tag{35}$$

$$\frac{\partial m}{\partial t} = K\theta \left(\frac{m}{m_i} \right)^{\alpha}(c-c_S) \quad . \tag{36}$$

The experimental conditions were selected so that θ and Q were constants in any given leaching column. The transport equations then reduce to:

$$\frac{\partial c}{\partial t} = D \frac{\partial^2 c}{\partial z^2} - U \frac{\partial c}{\partial z} - k \left(\frac{m}{m_i} \right)^{\alpha}(c-c_S) \tag{37}$$

$$\frac{\partial m}{\partial t} = k\theta \left(\frac{m}{m_i} \right)^{\alpha}(c-c_S) \quad . \tag{38}$$

Boundary and initial conditions on (37) and (38) which describe the experimental situation are:

$$-D \frac{\partial c}{\partial z} + Uc = 0 \qquad z=0 \quad , \quad t>0 \tag{39}$$

$$\frac{\partial c}{\partial z} = 0 \qquad z=L \quad , \quad t>0 \tag{40}$$

$$m(z,0) = m_i \tag{41}$$

$$c(z,0) = c_S \quad . \tag{42}$$

For convenience in comparison of the solution of (37) and (38) subject to the conditions (39) - (42) the following dimensionless variables were used:

$$T = Ut/L \qquad M = m/(\theta c_S)$$

$$Z = z/L \qquad G = Lk/U$$

$$C = c/c_S \qquad B = LU/D \quad .$$

Substitution of the dimensionless variables into Eqs. (37) through (42) gives:

$$\frac{\partial C}{\partial T} = \frac{1}{B} \frac{\partial^2 C}{\partial z^2} - \frac{\partial C}{\partial Z} - G \left(\frac{M}{M_i} \right)^{\alpha}(C-1) \tag{43}$$

$$\frac{\partial M}{\partial T} = G \left(\frac{M}{M_i} \right)^{\alpha}(C-1) \tag{44}$$

subject to:

$$\frac{\partial C}{\partial Z} - BC = 0 \qquad Z=0 \quad , \quad T>0 \tag{45}$$

$$\frac{\partial C}{\partial Z} = 0 \qquad Z=0 \quad , \quad T>0 \tag{46}$$

$$M(Z,0) = M_i \qquad 0 \leq Z \leq 1 \tag{47}$$

$$C(Z,0) = 1 \qquad 0 \leq Z \leq 1 \quad . \tag{48}$$

In the above $M_i = m_i/(\theta c_S)$.

The dimensionless time T represents the number of liquid filled pore volumes of solution that have passed through the column in physical time t . The Brenner number B is a measure of the relative importance of convection as compared to dispersion in a given column.

An analytic solution to (43) and (44) does not seem to be available, and numerical procedures were applied to obtain the solution. Several numerical methods were tried and compared. The first was finite difference method similar to that of Bresler (1973) designed to minimize numerical dispersion. The second was a variation of the method of characteristics, similar to that described by Smajstrla et al. (1973) (see also Garder et al., 1964). The third, the method of lines, utilized a program package called GEARB that was obtained from the Argonne National Laboratory, Agronne, Illinois. Additional details of these methods are available from the authors. [1]

---

[1] The Ph.D. dissertation by Tjaart Glas gives additional information on these methods and is available upon request.

CHAPTER V

RESULTS AND DISCUSSION

Dispersion Coefficient-Seepage Velocity Relationship

Dispersion coefficient data were obtained for the two soils by determining the best fit between measured chloride breakthrough curves and an analytical solution to Eq. (6) given by Brenner (1962). An optimization technique was used to minimize an objective function F by adjusting the parameters U and D in Brenner's solution. The optimization technique, first proposed by Powell (1964) and modified by Zangwill (1967) is available as the subroutine ZXPOWL in the International Mathematical Statistical Library. The objective function was defined as:

$$F = \sum_{i=1}^{n} (c_{i,0}-c_{i,p})^2/n \qquad (49)$$

where $c_{i,0}$ and $c_{i,p}$ are the observed and calculated values of the chloride concentration at a particular sampling time and n is the total number of samples for the chloride breakthrough curve.

The results of the dispersion coefficient and seepage velocity determinations by the optimization procedure are given in Table 3. As shown in Table 3, the values of U, calculated from the Darcy velocity, the bulk and particle densities, and the area of cross-section of the column, did not agree with the values of U obtained by optimization. These discrepancies are probably due in part to measurement errors, but are also due to the effect of anion exclusion especially in the case of the clay. The optimized seepage velocities for the clay soil were consistantly higher than those based on the Darcy velocity which would be the case if anion exclusion had occurred.

Figure 4 shows the dispersion coefficient-seepage velocity

Table 3. Results of the chloride breakthrough curve experiments.

Soil	Column Length	Solution Content	Bulk Density	Measured U	Two parameter optimization U	D	B	Fx10^2
	cm	cm^3/cm^3	g/cm^3	cm/hr	cm/hr	cm^2/hr		
Sand	30.0	0.25*	1.45	7.6	8.2	16.9	14.6	0.30
Sand	31.5	0.25*	1.59	6.6	8.2	24.8	10.4	0.26
Sand	30.0	0.28*	1.48	6.6	8.1	9.4	25.9	0.35
Sand	30.0	0.25*	1.50	8.4	8.0	13.3	18.2	0.21
Sand	31.5	0.25*	1.51	7.0	7.4	29.2	8.0	0.61
Sand	31.5	0.25*	1.51	4.5	5.8	17.0	10.7	0.31
Sand	30.0	0.25*	1.56	5.5	5.7	23.1	7.4	0.13
Sand	30.0	0.23*	1.51	5.0	5.4	17.3	9.4	0.29
Sand	30.0	0.27*	1.52	3.5	5.0	14.7	10.2	0.35
Sand	30.0	0.25*	1.40	5.4	5.0	2.4	62.5	0.17
Sand	30.0	0.25*	1.60	5.1	4.9	2.3	63.9	0.20
Sand	30.0	0.27*	1.52	3.8	4.1	6.7	18.4	0.37
Sand	30.0	0.41	1.56	3.4	3.6	3.8	28.5	0.07
Sand	30.0	0.41	1.56	3.1	3.2	4.0	24.0	0.02
Sand	30.0	0.41	1.56	3.1	3.7	5.3	20.9	0.05
Sand	30.0	0.41	1.56	2.5	3.0	3.9	23.1	0.06
Sand	30.0	0.41	1.56	1.9	2.0	2.2	27.3	0.03
Sand	30.0	0.40	1.58	1.3	1.8	1.8	30.0	0.01
Sand	30.0	0.41	1.56	1.2	1.4	1.5	28.0	0.08
Clay	31.0	0.52	1.24	2.3	3.7	7.3	15.7	0.19
Clay	32.5	0.52	1.24	1.5	2.6	3.9	21.7	0.01
Clay	31.0	0.50	1.32	1.4	2.3	6.4	11.1	0.07
Clay	31.0	0.49	1.35	1.2	1.9	4.3	13.7	0.16
Clay	32.5	0.52	1.24	1.0	1.8	2.9	20.2	0.04
Clay	32.0	0.50	1.32	0.9	1.5	1.1	43.6	0.06
Clay	30.0	0.48	1.38	0.9	1.5	4.2	10.7	0.30
Clay	30.0	0.47	1.40	1.0	1.2	2.5	14.4	0.05
Clay	32.0	0.50	1.32	1.0	1.2	1.7	22.6	0.06
Clay	30.0	0.49	1.35	0.6	0.9	1.0	27.0	0.18
Clay	32.5	0.52	1.24	0.6	0.7	1.4	16.3	0.07

In the experiments indicated by the symbol * the solution content θ was smaller than the saturated solution content θ_s .

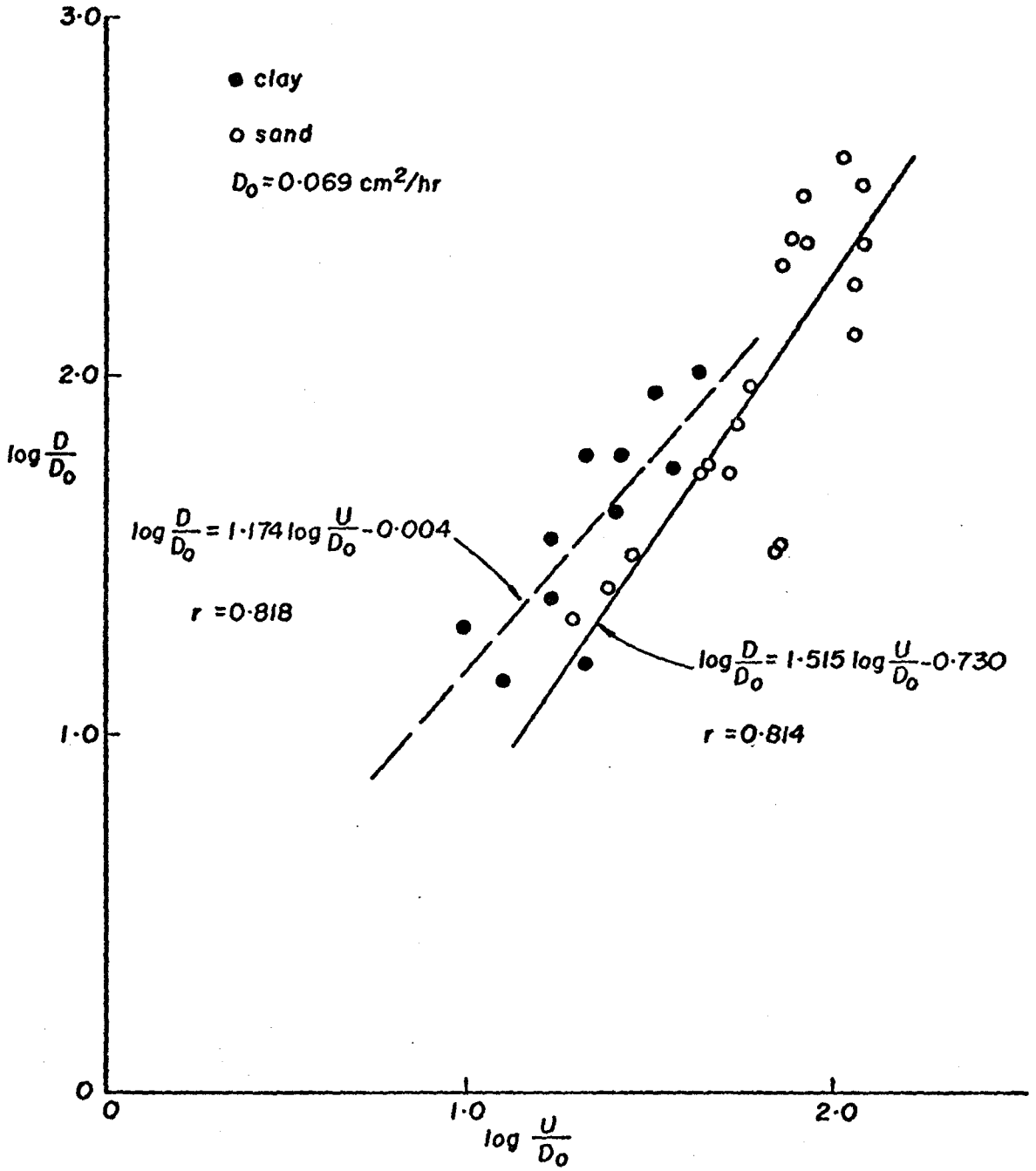

Fig. 4. Dispersion coefficient - seepage velocity relationship for the sand (solid line) and the clay (dashed line).

relationship for the sand and clay, as well as the results of linear regressions using the form:

$$\text{Log}\left(\frac{D}{D_0}\right) = m\ \text{Log}\left(\frac{U}{D_0}\right) + b \qquad (50)$$

where m and b are the slope and intercept of the linear log (D/D_0) versus $\log(U/D_0)$ relationship. The molecular diffusivity D_0 used in this regression was that for KCl which is $0.069\ cm^2/hr$ at $25°C$. The regression equations given in Fig. 4 were used to calculate dispersion coefficients for the gypsum leaching experiments.

Properties of the Gypsum Material

Table 4 gives the calcium concentrations of solutions equilibrated with an excess of the gypsum material by shaking for 168 hours. Duplicate measurements A and B were made on each size range. These results show no systematic differences between the size ranges and duplicates, and are within the range of measured solubilities for gypsum in distilled water as reported in the literature. Based on the results in Table 4 the concentration scaling factor c_s was set equal to 30.5 meq/l.

The purity of the gypsum material was studied by shaking less than an excess of the material in distilled water. The calcium and sulfate concentrations in the resulting solutions differed by less than 10 percent in terms of milliequivalents per liter, indicating that the main source for calcium and sulfate in the solution was solid phase gypsum. The magnesium concentration in all of the samples was less than 0.01 meq/l. Assuming that the solid phase gypsum was the only source of calcium in the solution, the amount of pure gypsum was calculated from the calcium concentrations in the solutions. These results for the different size fractions are shown in Fig. 5. The amount of pure gypsum ranges from

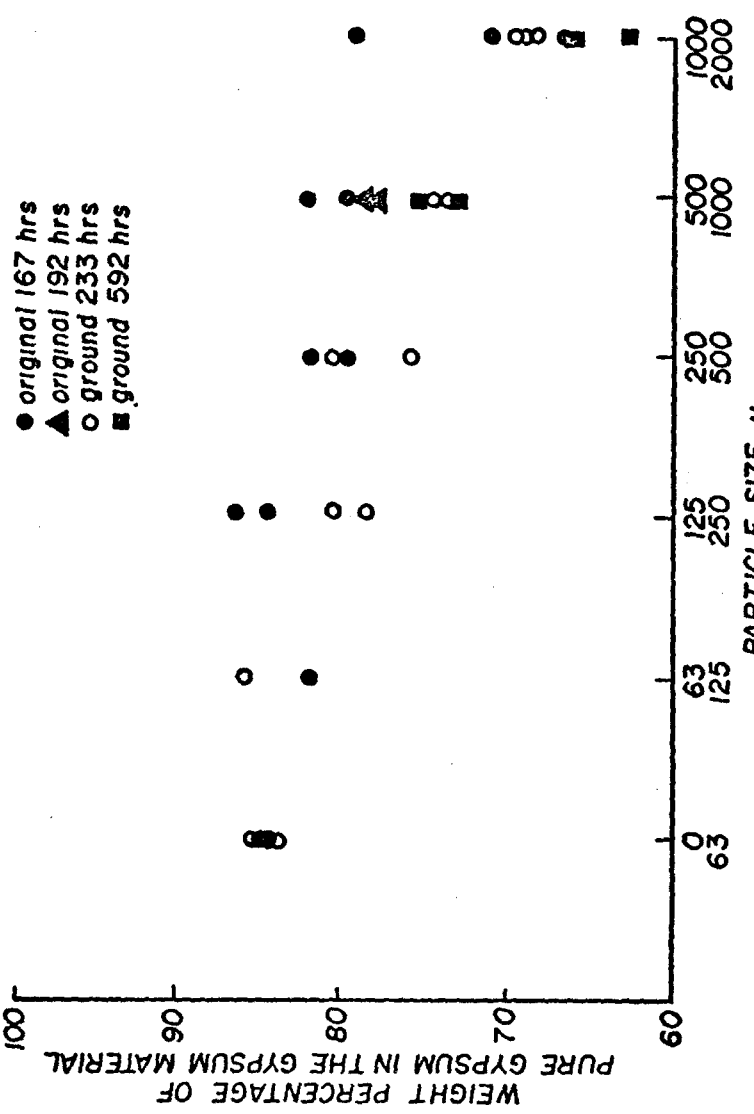

Fig. 5. Purity of the gypsum material as a function of particle size.

Table 4. Calcium concentrations (meq/l) in solutions saturated with solid phase gypsum material of the six different size ranges.

Ca^{2+} (meq/l)	Size ranges (μ)						Average Ca^{2+} conc. (meq/l)
	0 - 63	63 - 125	125 - 250	250 - 500	500 - 1000	1000 - 2000	
A	29.8	31.2	30.1	31.0	30.5	29.7	30.4
B	31.6	30.6	29.7	29.9	30.0	36.1	30.6

about 85 percent for the finest particle size class to approximately 65 percent for the 1-2 mm size range. The scatter in the data are attributed to the nonuniformity of sub-samples of the gypsum material. Table 5 gives the carbonate content of the different size ranges and the white, yellow and black fractions of the 1-2 mm material. From the data in Table 5 and Fig. 5 it appears that pure gypsum and carbonates account for 80-90 percent of the gypsum material. It was found in the shaking studies that part of the material was insoluble in water. Analyses showed this insoluble material to consist mainly of silica and iron compounds.

The results of the dissolution rate study for the various particle sizes are shown in Fig 6. The calcium concentration is plotted versus shaking time. The smallest size ranges were apparently dissolved within 1 hour, but the two largest size ranges showed significant increases in calcium concentration up to 6 hours of shaking time. These shaking study results are not useful as a measure of the rate of solution in a porous medium because of the different conditions under which the dissolution occurs. In a shaking study the dissolved material is swept away by turbulence in the solution, while in a soil-water system the transport away from the particle surface is by a slower laminar convection and diffusion process. However, the results of the shaking studies indicate

that at least for the larger particles it will not be possible to describe the dissolution as an equilibrium process.

Table 5. Carbonate content (% by weight) in the different size ranges and separated fractions of the gypsum material.

	Size range (μ)						Fraction of 1-2 mm material		
	0-63	63-125	125-250	250-500	500-1000	1000-2000	white	yellow	black
% carbonate	3.6	2.0	2.3	5.4	10.1	14.7	0.7	13.0	32.5

Gypsum Leaching Results

Tables 6 and 7 summarize the physical parameters of the various gypsum leaching experiments for the sand and clay respectively.

Experiments in which the solution content was less than the saturation value are indicated with the symbol + . It was attempted in these experiments to maintain the solution content constant with respect to position and time. The tensiometer readings indicated that this goal was not completely attained. In general the tensiometer readings varied with respect to elevation as well as time. The differences with respect to elevation corresponded to an absolute solution content variation of up to 10 percent. In most cases the solution content increased with depth. It was found that the solution contents inferred from the tensiometer readings and the pressure head-solution content relationships in Fig. 1 were not the same as those obtained from gravimetric determinations at the end of the experiment, probably because of packing differences between the column and the samples used to obtain the data in Fig. 1. It was decided to use the average of the solution contents determined at the end of each experiment under unsaturated conditions as the solution content for modeling purposes. In the saturated columns the total porosity was calculated from the bulk and particle densities.

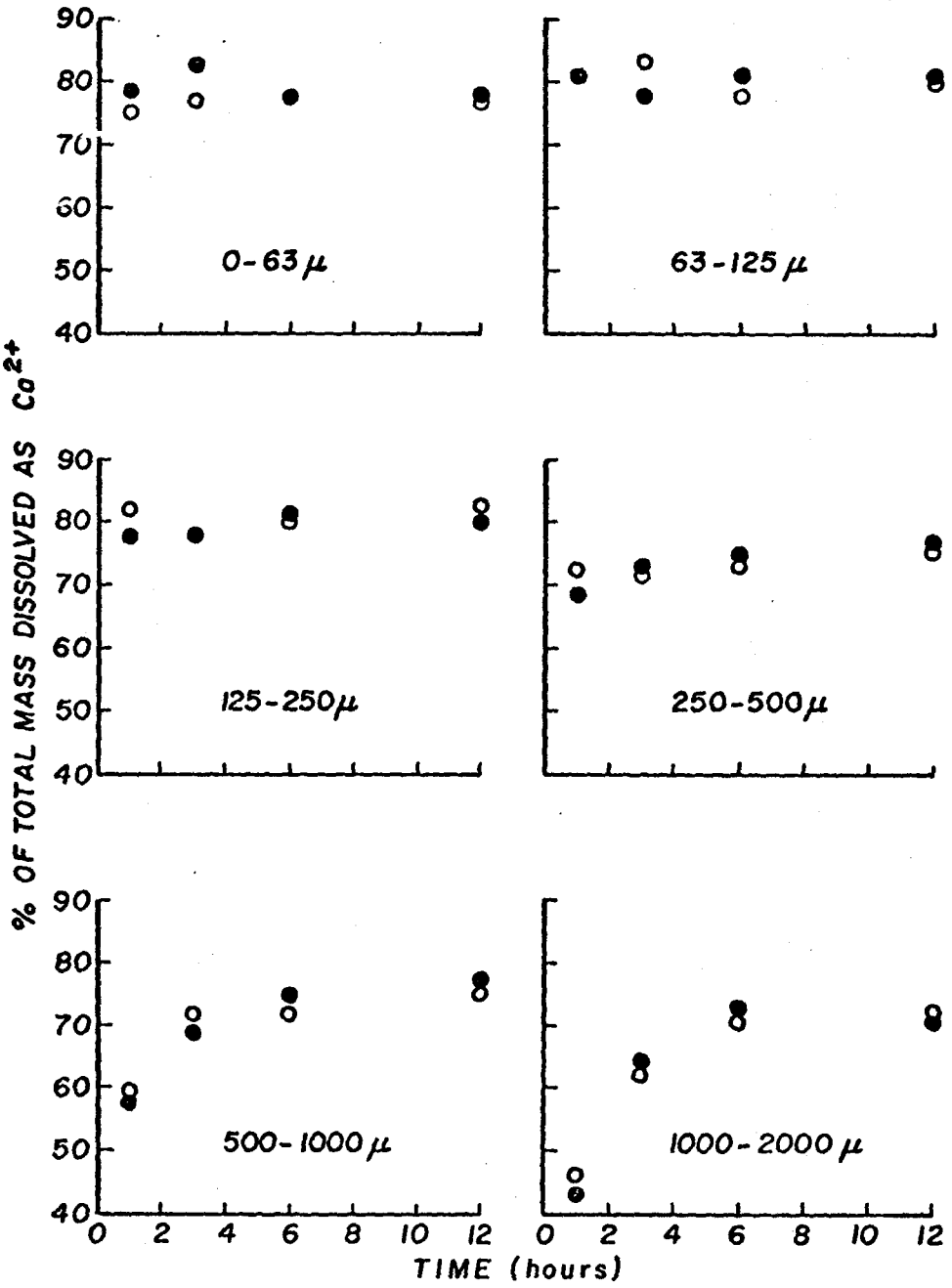

Fig. 6. Percentage of the total mass of gypsum material dissolved in water as a function of the shaking time. The black dots and open circles represent results from duplicate experiments.

Table 6. Physical parameters of the gypsum leaching studies performed in the sand.

Experiment No.	L	A_c	θ	β	U	B	$m_{i,tot} \times 10^3$	Particle Size
	cm	cm^2	cm^3/cm^3	g/cm^3	cm/hr		g/cm^3 p.m.	μ
1	28.0	37.8	0.42	1.55	1.31 ± 0.20	33.0	15.7	63-125
2	28.0	37.8	0.38	1.64	1.45 ± 0.25	31.3	16.7	63-125
3	30.0	31.2	0.41	1.57	1.93 ± 0.25	29.0	15.8	63-125
4	28.0	37.8	0.41	1.56	2.82 ± 0.30	22.2	16.0	63-125
5	31.5	176.7	0.25+	1.51	5.80 ± 1.10	17.3	15.3	63-125
6	29.0	37.8	0.40	1.55	11.99 ± 0.35	10.9	15.7	63-125
7	30.0	176.7	0.27+	1.52	3.44 ± 0.55	30.0	15.3	125-250
8	33.5	31.2	0.42	1.55	1.44 ± 0.50	37.6	15.6	250-500
9	28.0	37.8	0.41	1.57	1.99 ± 0.35	26.6	16.0	250-500
10	30.0	176.7	0.27+	1.52	3.81 ± 0.35	20.4	15.5	250-500
11	28.5	37.8	0.40	1.55	4.02 ± 1.25	18.9	15.8	250-500
12	10.0	60.8	0.41	1.55	0.14 ± 0.03	36.8	15.6	500-1000
13	29.0	37.8	0.38	1.65	1.21 ± 0.02	35.6	16.7	500-1000
14	30.0	176.7	0.28+	1.52	6.21 ± 0.90	15.9	29.4	500-1000
15	29.0	37.8	0.37	1.66	11.34 ± 2.70	11.3	15.5	500-1000
16	28.5	37.8	0.39	1.63			16.4	500-1000
17	28.0	37.8	0.38	1.64	1.24 ± 0.10	34.0	16.5	1000-2000
18	30.0	176.7	0.25+	1.53	1.74 ± 0.60	30.6	14.9	1000-2000
19	28.5	37.8	0.43	1.52	2.34 ± 0.25	24.9	15.8	1000-2000
20	30.0	31.2	0.38	1.65	2.66 ± 0.30	24.6	16.7	1000-2000
21	31.5	37.8	0.37	1.64	8.11 ± 1.35	14.5	16.0	1000-2000
22	30.0	176.7	0.23+	1.51	4.50 ± 0.60	18.7	15.3	1000-2000
23	27.5	37.8	0.38	1.63	1.47 ± 0.20	30.6	8.3	Precipitated
24	30.0	37.8	0.36	1.70	1.58 ± 0.35	32.1	8.5	Precipitated
25	30.0	31.2	0.37	1.66	2.73 ± 0.35	24.2	8.3	Precipitated
26	30.0	37.8	0.36	1.69	6.30 ± 0.55	15.8	8.5	Precipitated
27	30.0	31.2	0.39	1.64	1.46 ± 0.40	37.6	18.4	Reagent Grade

+ Solution content θ smaller than the saturated solution content.

Table 7. Physical parameters of the gypsum leaching studies performed in the clay.

Experiment No.	L	A_c	θ	β	U	B	$m_{i,tot} \times 10^3$	Particle Size
	cm	cm^2	cm^3/cm^3	g/cm^3	cm/hr		g/cm^3 p.m.	μ
28	31.5	176.7	0.55	1.21	0.13 ± 0.02	28.5	6.0	0-63
29	31.0	37.8	0.50	1.34	0.26 ± 0.05	24.8	13.7	0-63
30	28.0	37.8	0.55	1.21	1.97 ± 0.15	15.8	13.8	0-63
31	30.0	176.7	0.51	1.32	0.18 ± 0.10	25.6	12.8	63-125
32	30.0	37.8	0.53	1.25	0.83 ± 0.10	19.6	12.6	63-125
33	28.5	37.8	0.48	1.40	0.98 ± 0.10	18.1	13.8	63-125
34	30.5	37.8	0.54	1.24	2.07 ± 0.50	17.0	12.3	63-125
35	31.0	176.7	0.53	1.26	0.51 ± 0.10	22.1	6.2	125-250
36	28.5	37.8	0.47	1.42	0.55 ± 0.10	20.0	14.1	125-250
37	30.0	176.7	0.53	1.26		23.7	6.2	250-500
38	30.0	176.7	0.51	1.32	0.29 ± 0.10	23.6	6.6	250-500
39	31.0	176.7	0.42+	1.29	0.35 ± 0.05	21.6	6.4	250-500
40	30.5	37.8	0.46	1.45	1.37 ± 0.30	18.3	14.5	250-500
41	28.0	37.8	0.47	1.42	2.00 ± 0.50	15.7	14.1	250-500
42	32.0	176.7	0.42+	1.22	0.33 ± 0.10	24.6	6.2	500-1000
43	31.0	176.7	0.52	1.29	0.81 ± 0.10	20.4	6.2	500-1000
44	31.0	176.7	0.41+	1.25	0.10 ± 0.05	29.3	6.3	1000-2000
45	31.0	176.7	0.53	1.26	0.41 ± 0.15	22.9	6.3	1000-2000
46	30.0	37.8	0.49	1.37	0.49 ± 0.20	17.9	13.2	1000-2000
47	30.0	31.2	0.50	1.34	1.92 ± 0.25	17.0	13.4	1000-2000
48	28.0	37.8	0.53	1.26	1.74 ± 0.20	16.1	5.6	Precipitated
49	30.0	37.8	0.54	1.24	3.90 ± 1.0	15.0	6.2	Precipitated
50	31.0	37.8	0.47	1.42	0.91 ± 0.15	19.3	22.2	Reagent Grade

+Solution content θ is smaller than the saturated solution content.

The seepage velocities calculated from the measured Darcy velocity and solution content ranged from 0.14 to 11.99 cm/hr in the sand, and from 0.10 to 3.90 cm/hr in the clay. The error bounds on U shown in Tables 6 and 7 were calculated from the measured fluctuations in the Darcy velocity. Usually these fluctuations were within 25 percent of the average. In experiments 16 and 37 the flow rate was purposely varied with time by turning off the inflow pump during certain time periods.

The Brenner number B, which varied from 10.9 to 37.6 in the sand and from 15.0 to 29.3 in the clay, was calculated from the relationship $B=LU/D$. The dispersion coefficients were obtained from the seepage velocities using the regression equations given in Fig. 4.

The results of the experiments conducted to test the uniformity of the initial soil-gypsum mixture are shown in Fig. 7. The mass of calcium recovered in the solution samples expressed as a percentage of the total mass of gypsum material added is plotted against depth. The scatter in the data in the experiments in which natural gypsum material was used could be due to nonuniformity of the gypsum material or to nonuniformity of the mixture. The bottom graph in Fig. 7 shows that an almost uniform gypsum distribution was obtained by using reagent grade gypsum in the mixture. Accordingly, it is believed that the scatter in the case of the natural material is largely due to the nonuniformity of the material.

The sand contained about 0.1 percent of carbonates (see Table 2). When a sand column (without gypsum) was leached with distilled water at a Darcy velocity of about 1.5 cm/hr it was found that the calcium concentration in the effluent and suction cup solution samples was less than 1 meq/l. Although the carbonates were removed by acid washing in some of the experiments, their presence was neglected in all cases.

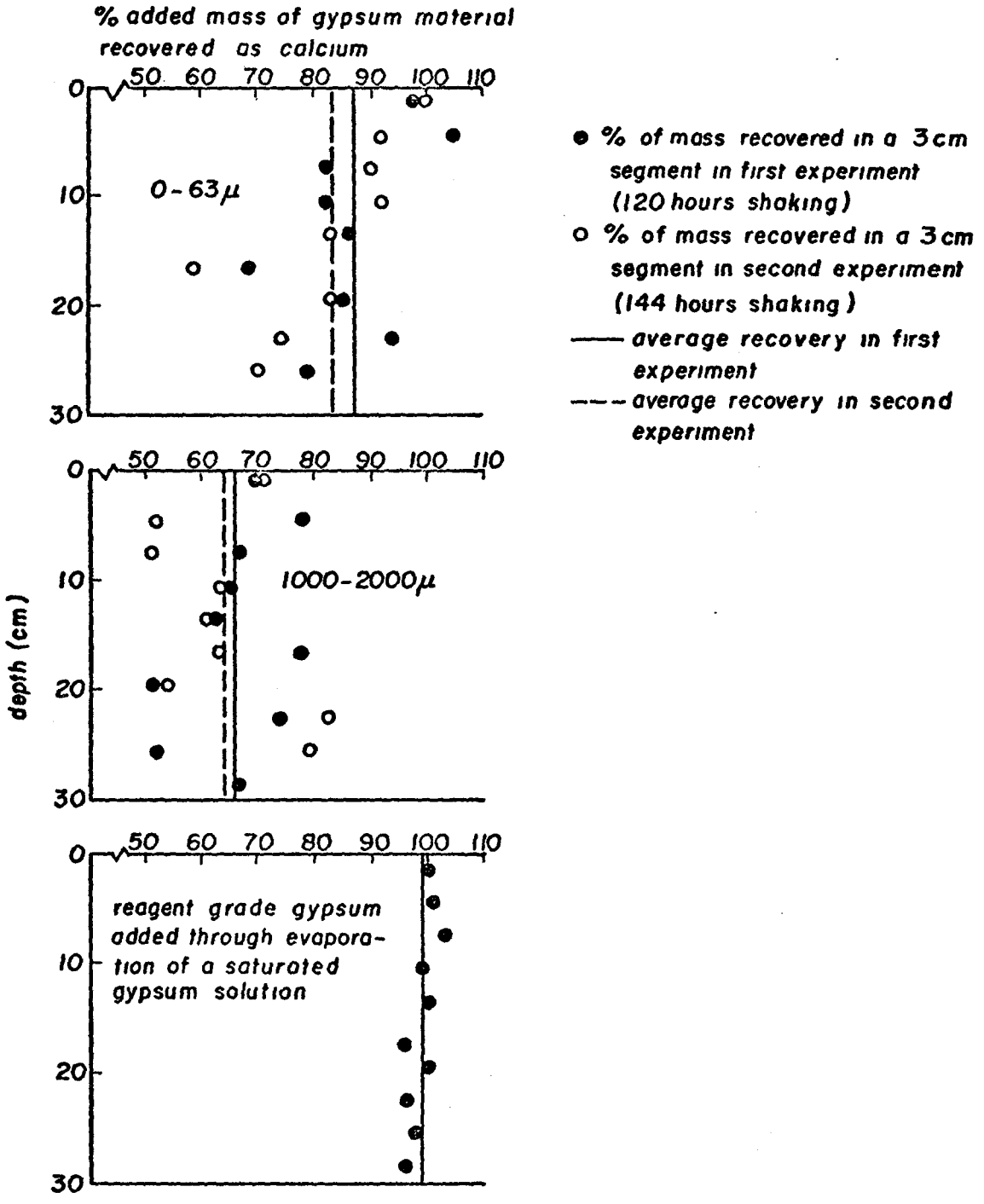

Fig. 7. Uniformity of the initial soil-gypsum mixture.

In two experiments (Nos. 20 and 36) the calcium and sulfate concentrations were measured in the solution samples. The generally good agreement between the calcium and sulfate concentrations versus time shown in Figs. 8 and 9 indicates that the main source of calcium in the solution was the gypsum and that the carbonates present in the gypsum material contributed little calcium to the solution.

The concentration-time curves shown in Figs. 8 and 9 are representative of the two types of curves obtained in the experiments. In certain cases as shown in Fig. 9, the concentration remained at the saturation value for some time before gradually decreasing with time. Some of the curves, e.g., that for $z=0.30$ in Fig. 9, resemble breakthrough curves. However, the inflection point of the observed curves occurred at pore volume values (dimensionless time) far too large to be due to dispersion. In general, the number of pore volumes of leaching required to bring about a decrease in the calcium concentration was mainly determined by the amount of solid phase gypsum added.

Predictions of the Mixing Cell Model

In order to explore the characteristics of the predictions of the mixing cell model, the model was applied in some hypothetical situations. In the first, a column of salt that contained no solid phase gypsum, with a solution phase concentration that was constant and equal to c_0, was leached with distilled water. No reactions were considered to occur and the change in concentration with time was calculated from Eq. (21). The effect of the chosen magnitudes of the depth and time increments on the calculated breakthrough curves is shown in Fig. 10. An increase in Δz or a decrease in Δt caused the concentration to decrease more gradually with time in a manner suggestive of the dispersion process. This

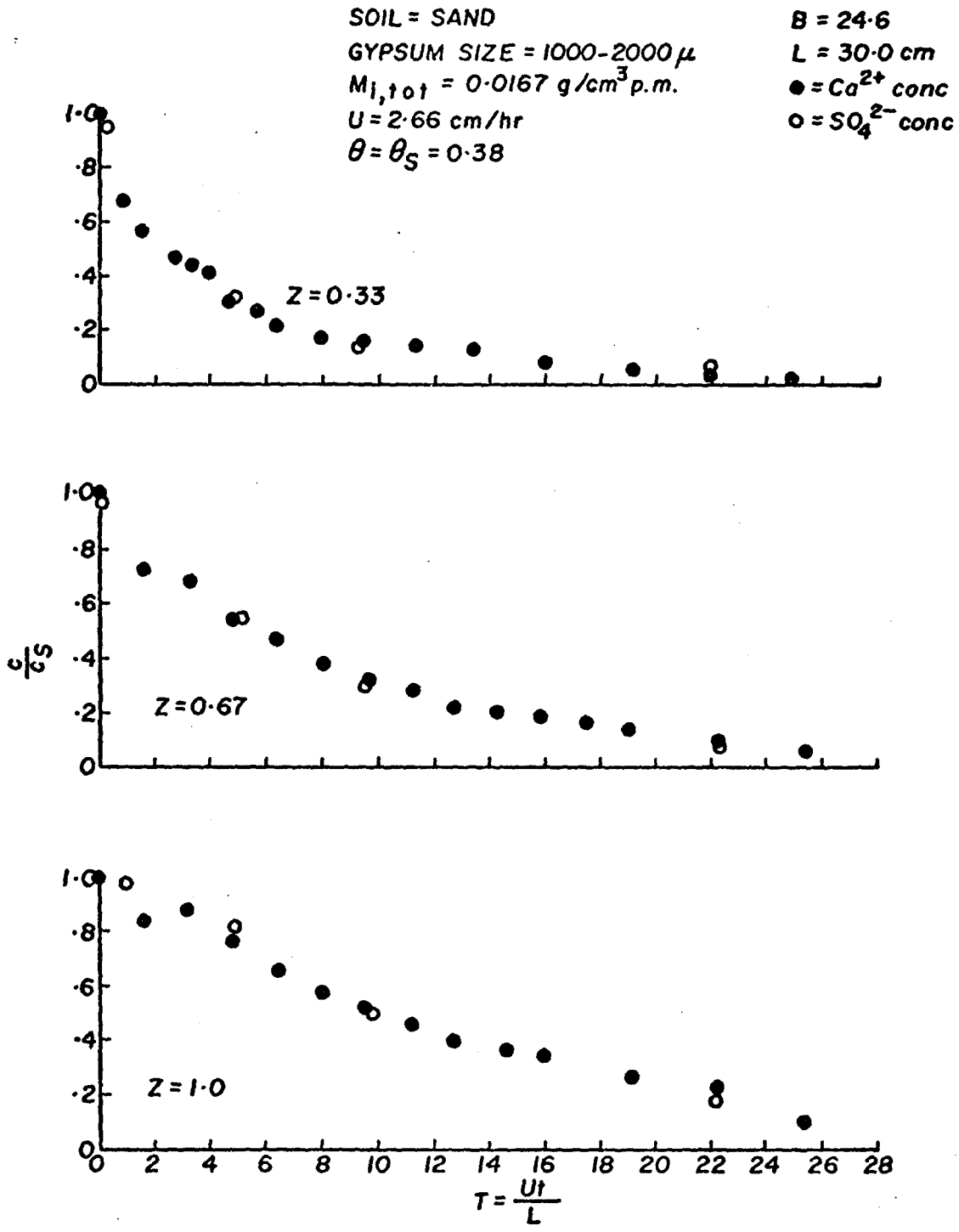

Fig. 8. Measured dimensionless concentration of calcium (black dots) and sulfate (open circles) in the solution phase against dimensionless time for experiment 20.

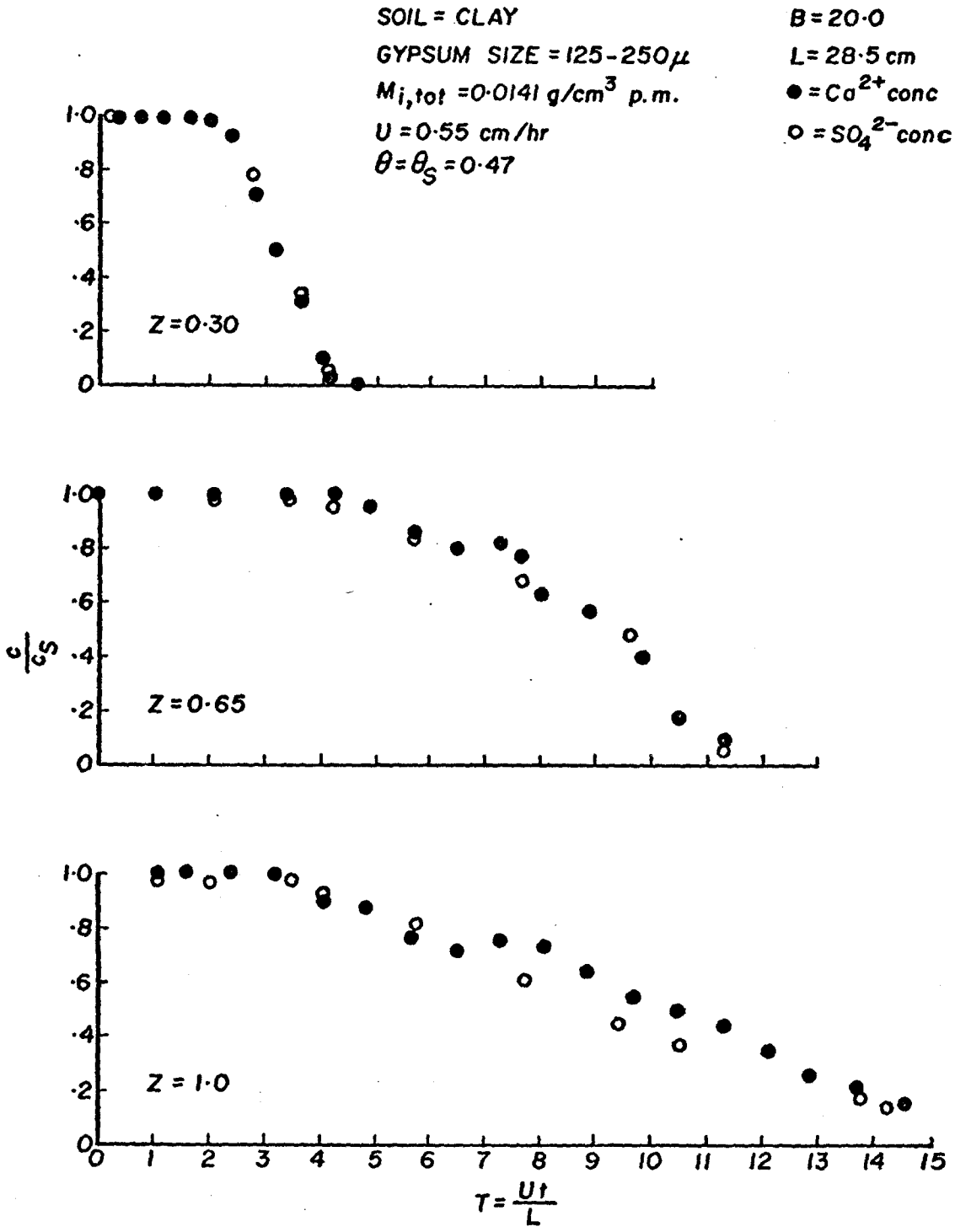

Fig. 9. Measured dimensionless concentration of calcium (black dots) and sulfate (open circles) in the solution phase against dimensionless time for experiment 36.

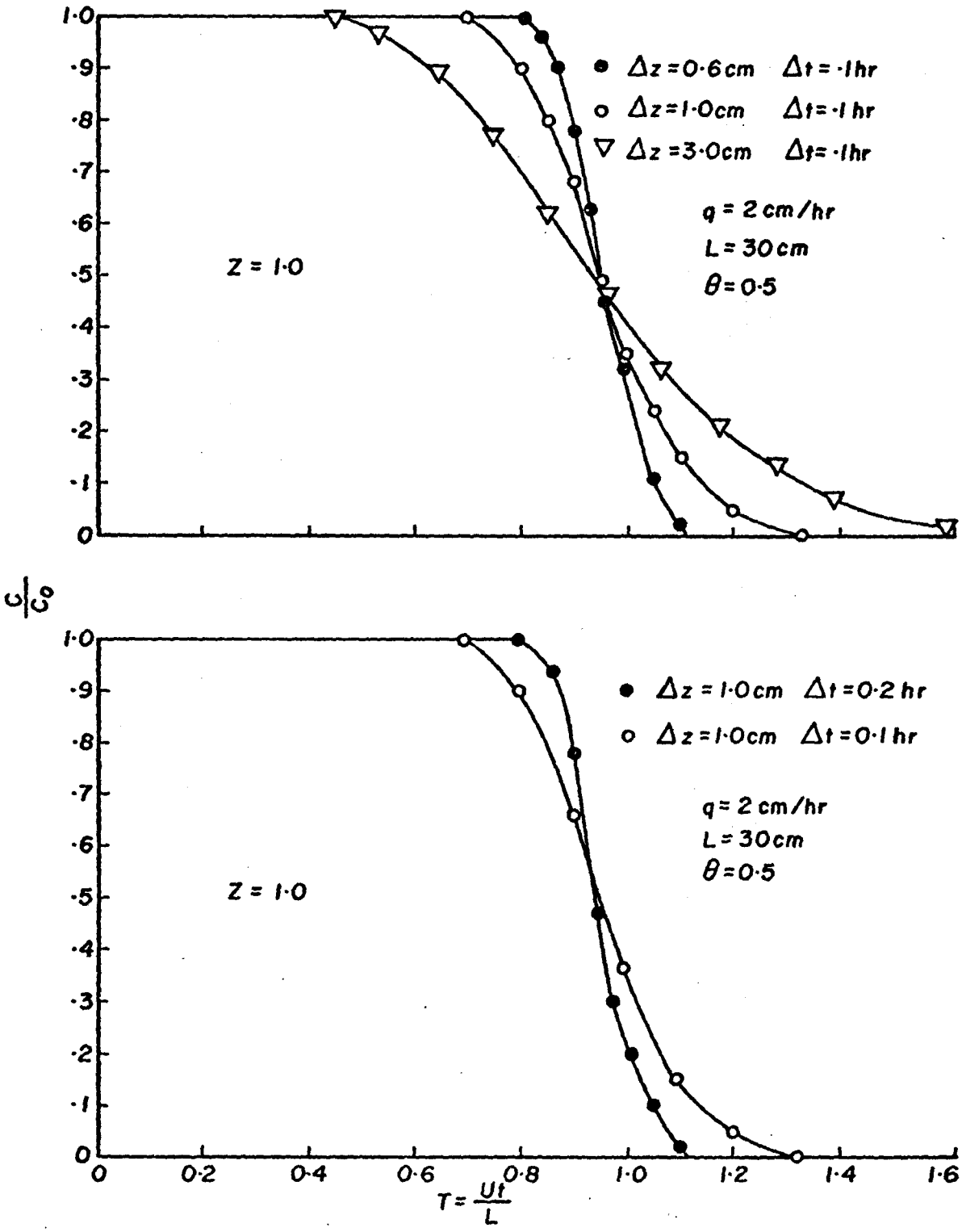

Fig. 10. The effect of the magnitude of the time step and depth increment on the shape of breakthrough curves calculated with the mixing cell model.

"built in" numerical dispersion has no physical meaning but it has been used to simulate the dispersion process (e.g., Tanji et al., 1967; Dutt et al., 1972).

The results of a simulation of the leaching of solid phase gypsum from a column are shown in Fig. 11. The calculated concentration-time curves resulting from the mixing cell model are step like due to the fact that the solution phase concentration remains equal to the saturation value as long as there is solid phase gypsum in the region above the depth at which the concentration-time curve is calculated. As soon as all the solid phase gypsum in the region is dissolved the concentration drops to zero. There is a small effect of the numerical dispersion on the results, but it is not large enough to change the basic shape of the step front type curves.

The physical time at which the concentration drops to zero can be estimated from mass balance principles in which the total mass of gypsum to be dissolved and displaced is equated to the initial amount of solid phase and solution phase gypsum in the column in a region of depth z_d. On a unit cross-sectional area basis we can write

$$c_S q t_d = z_d m_i + z_d \theta c_S$$

which can be solved for t_d:

$$t_d = z_d \left(\frac{m_i}{c_S q} + \frac{\theta}{q} \right) \quad . \tag{51}$$

In terms of dimensionless variables this becomes:

$$T_d = Z_d (M_i + 1) \quad . \tag{52}$$

The dimensionless times for the occurrence of the step decrease in concentration at a given depth calculated from Eq. (52) agree with those

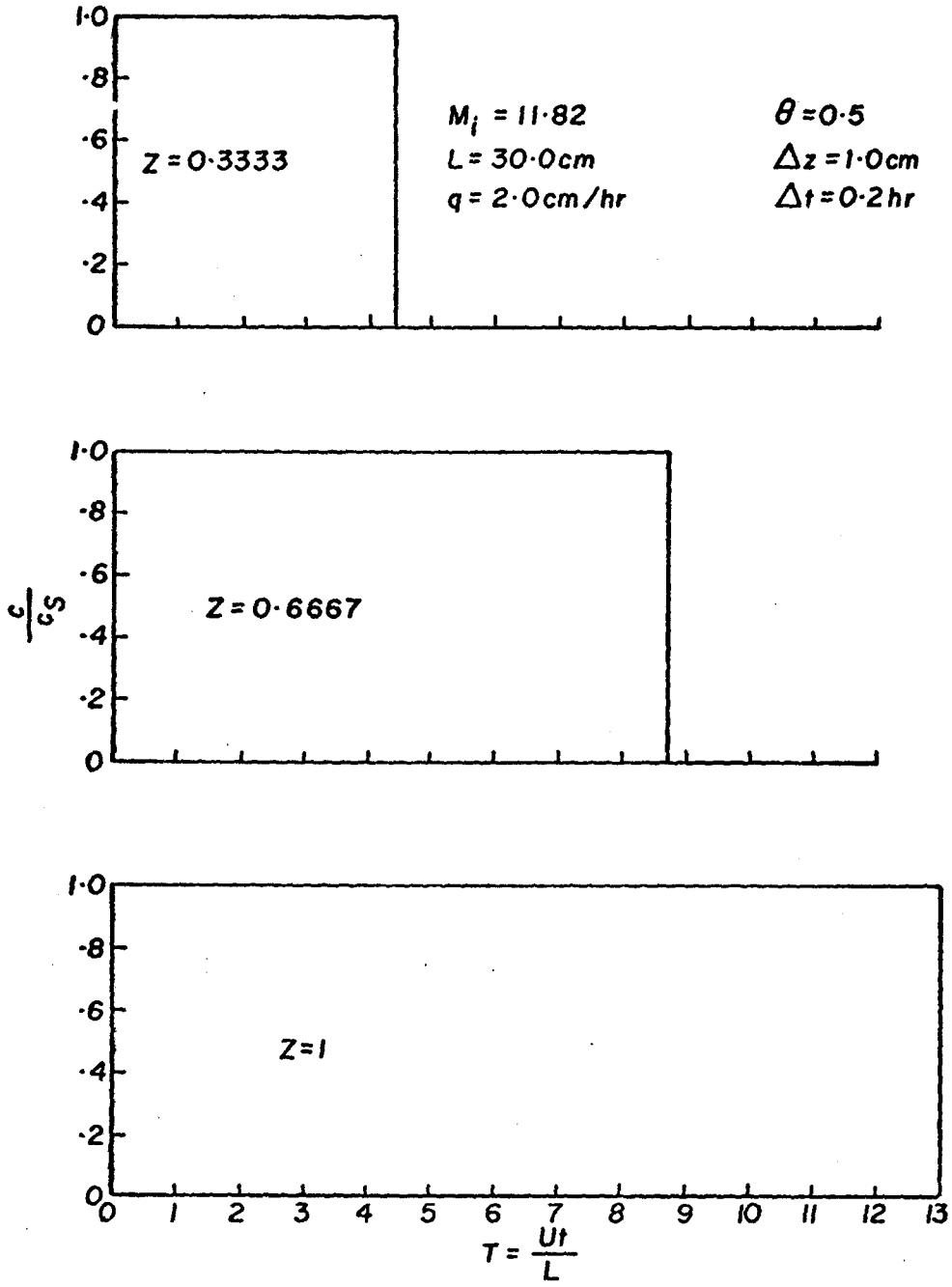

Fig. 11. Concentration-time curves at three different positions calculated with the mixing cell model.

calculated from the mixing cell model except for small uncertainties due to the numerical dispersion effect in the latter.

Predictions of the Kinetic Model

The effect of the various parameters in the transport equation on the concentration-time curves was examined in a series of computer solutions. These results are shown in terms of dimensionless variables in Figs. 12, 13, 14 and 15. Figure 12 displays the effect of the Brenner number. A decrease in B, corresponding to an increase in the ratio of the dispersion coefficient to the seepage velocity, causes the curves at all positions to become flatter. The effect on the effluent curve is smaller than on the two curves at the internal positions. This is due to the action of "back-dispersion", i.e., a flux component proportional to the concentration gradient, which is present at the internal positions, but is not present at the outlet boundary. The outlet boundary condition is one of zero concentration gradient.

The dimensionless reaction rate parameter has a marked effect on the shape of the curves at all positions (Fig. 13). As G is increased from 2.5 to 30 the curves change from a concave to a convex shape. At smaller values of the reaction rate parameter the reaction does not proceed fast enough to keep the concentration in the solution phase equal to c_S, and the tail on the curves is longer.

An increase in the exponent α increases the tailing but does not greatly change the shape of the curves (Fig. 14). As α increases the rate of dissolution decreases more than linearly with a decrease in the mass of solid phase gypsum.

Figure 15 shows that an increase in M_i, corresponding to an increase in the amount of solid phase gypsum, causes the curves to shift to the right.

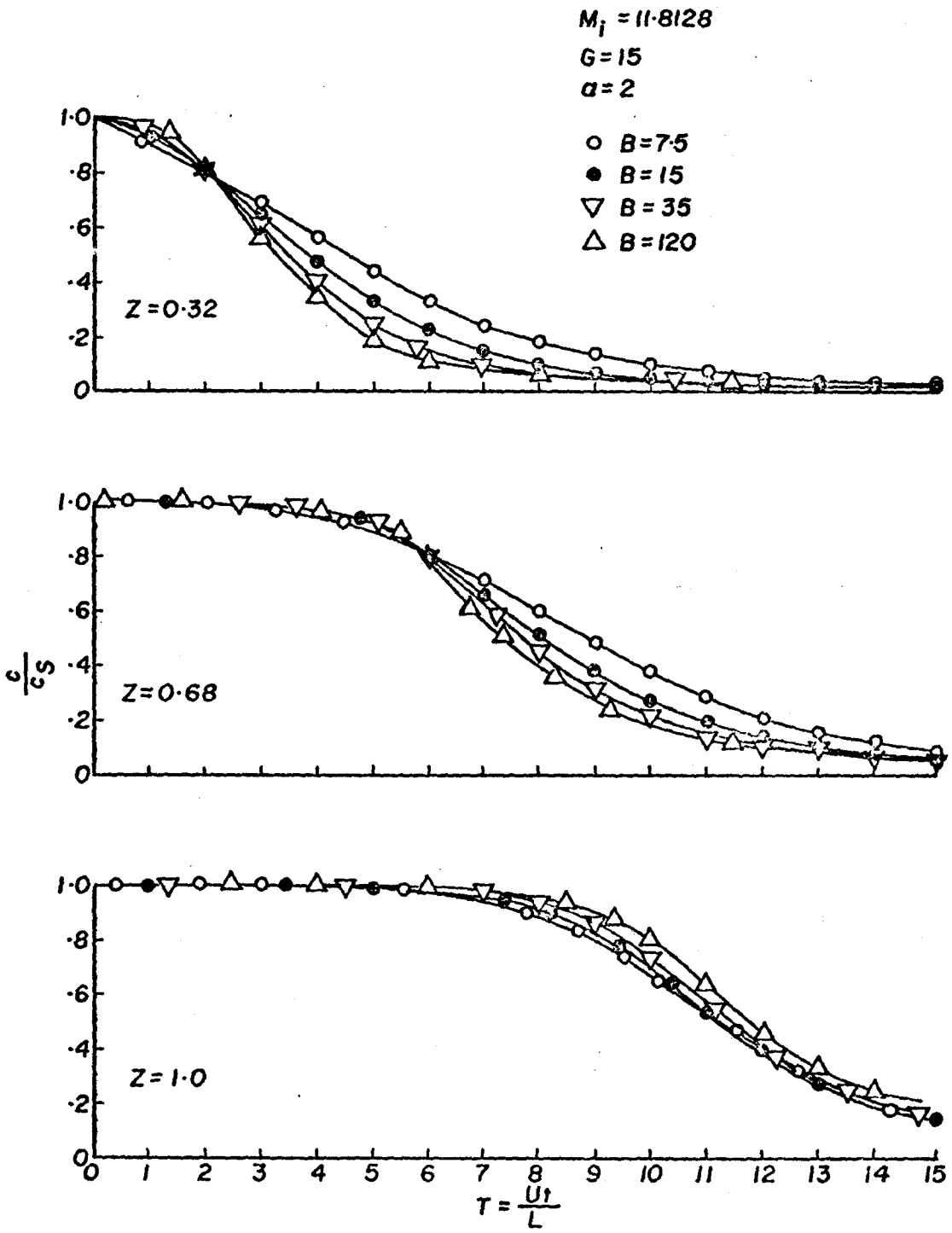

Fig. 12. The effect of the Brenner number B in the kinetic model.

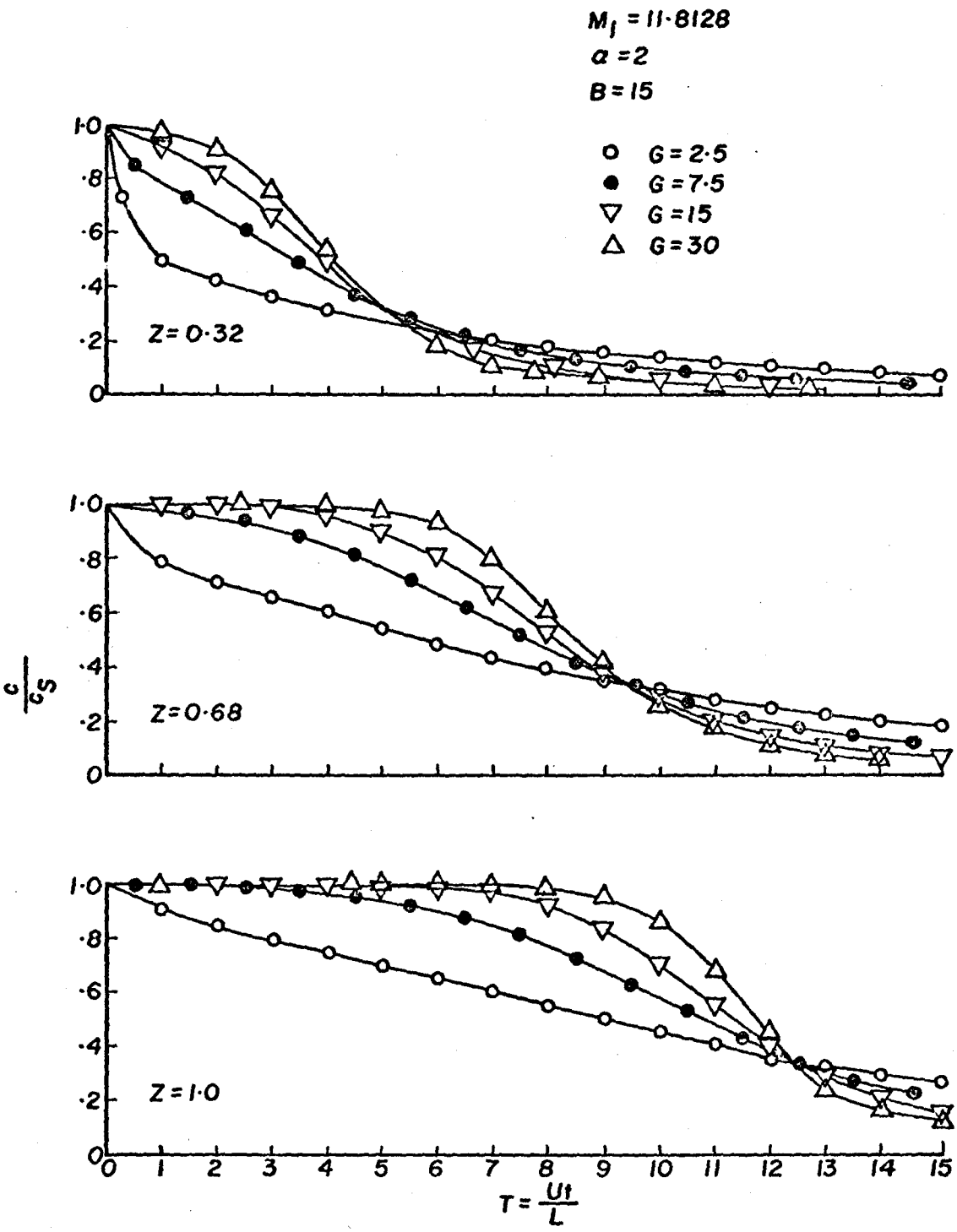

Fig. 13. The effect of the dimensionless reaction rate parameter G in the kinetic model.

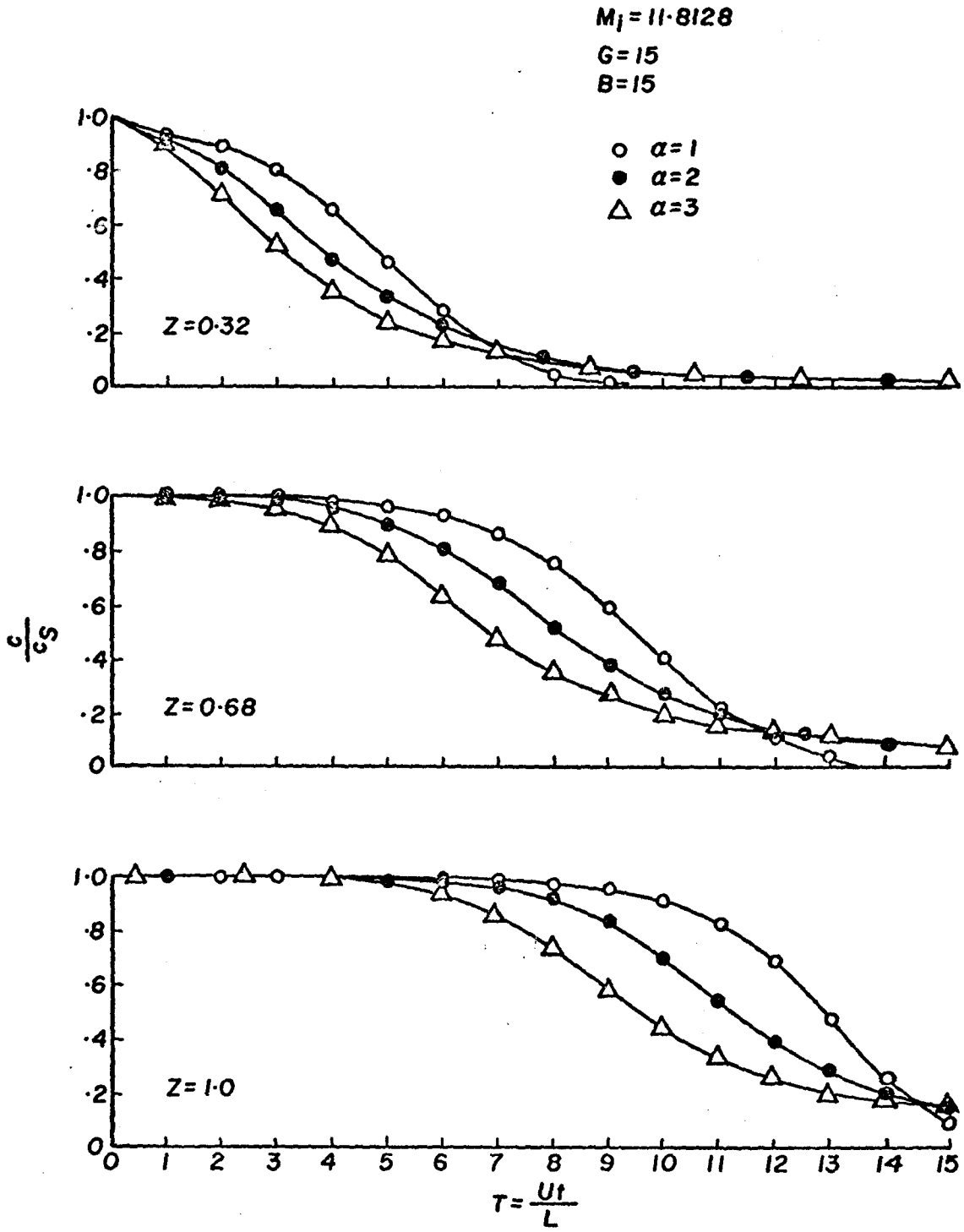

Fig. 14. The effect of the parameter α in the kinetic model.

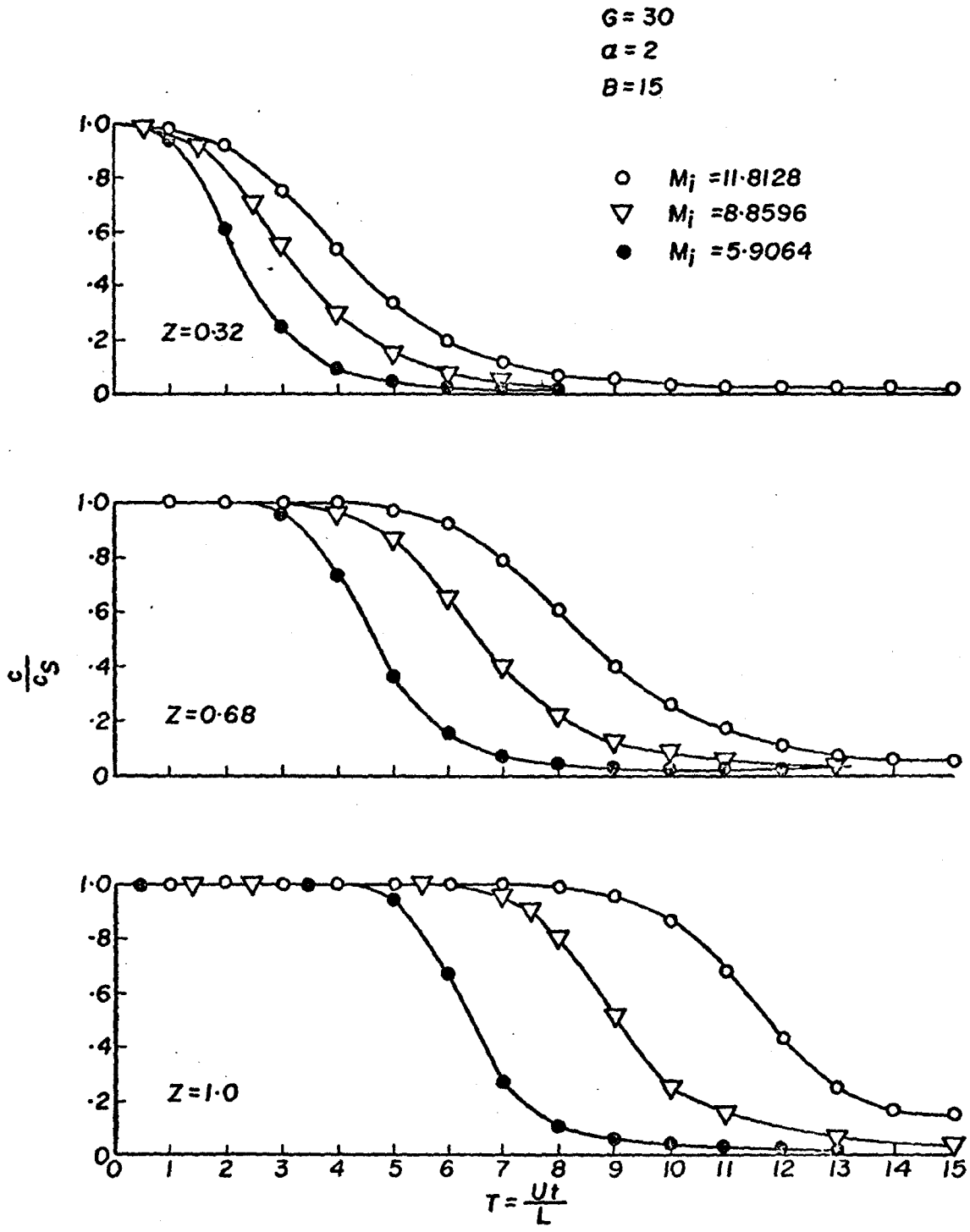

Fig. 15. The effect of the initial dimensionless mass of gypsum M_i in the kinetic model.

In the gypsum leaching studies a variation of solution content with depth was observed. Figure 16 shows the effect of a linear variation of θ with z on the concentration time curves as calculated from the kinetic model. It appears that a variation of θ of about 10 percent would not significantly affect the time dependence of the concentration. In the leaching studies, a time variation of the seepage velocity was also observed. Figure 17 shows the calculated effect of a Darcy velocity that varies linearly with time on the concentration-time curves. Also shown is the concentration-time curve for a constant Q equal to the time integrated mean of the varying velocity. A systematic change in Q of the magnitude shown in Fig. 17 produces a significant shift in the curves. However, a systematic change of this magnitude was not found in the experiments. It was much more typical for Q to vary in a fluctuating manner. Figure 18 shows the effect of a hypothetical fluctuation in Q of $\pm$ 20 percent of the mean value of Q on the concentration-time curves. In this case the concentration fluctuates to some extent on either side of the curve for constant Q. Another problem observed in the leaching experiments was the nonuniformity of distribution of the natural solid phase gypsum (see Fig. 7). In Fig. 19 concentration-time curves for a variable distribution of solid phase gypsum are shown, and compared to the results for a constant distribution of M_i. It was concluded that the deviations from nonuniformity of distribution of solid phase gypsum of the kind shown in Fig. 19 did not significantly affect the measured concentration-time curves.

Comparison Between the Gypsum Leaching Studies and the Models

Parameters for the kinetic model - In preliminary attempts to compare experimental data with calculated results, large deviations were

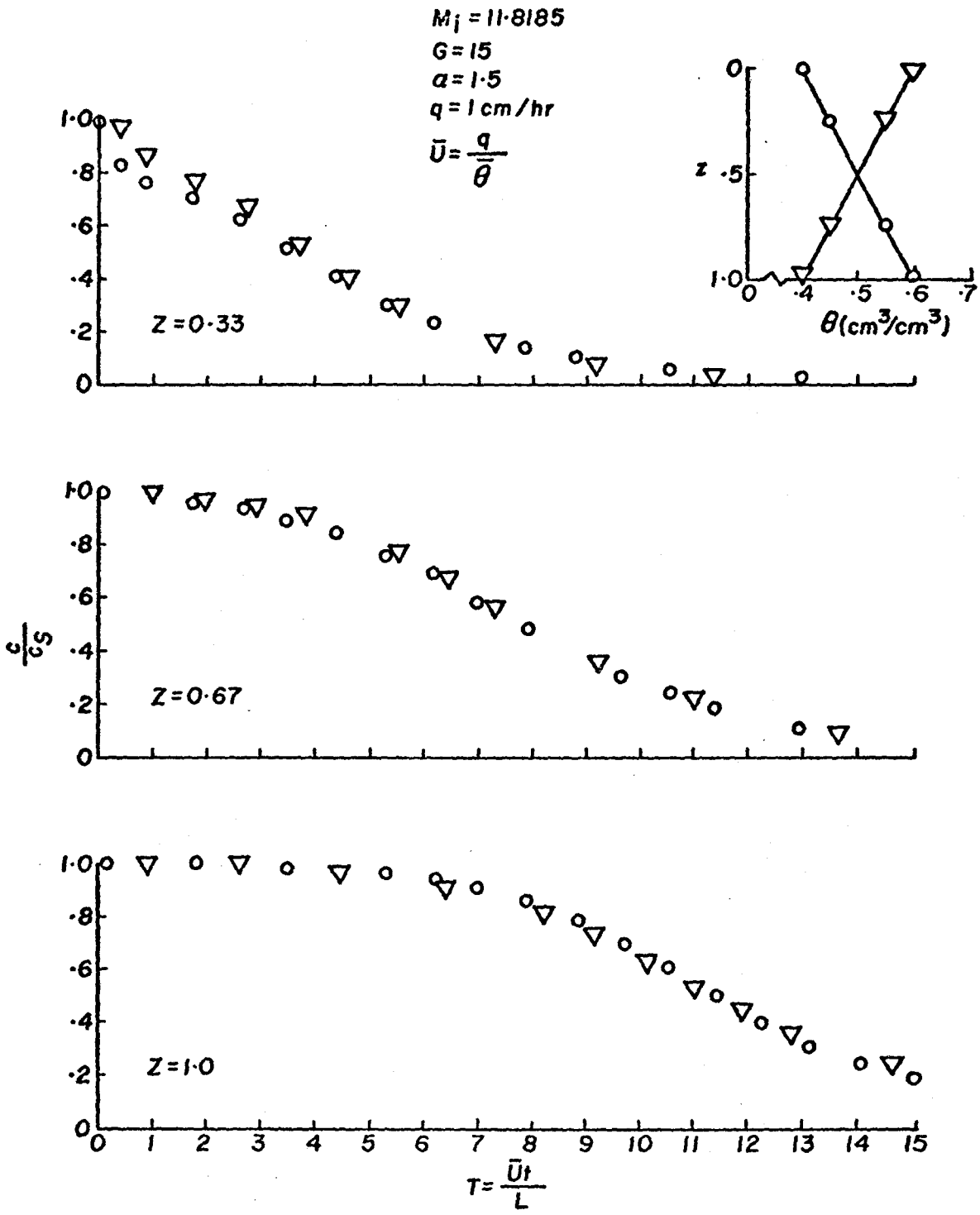

Fig. 16. The effect of a variation of the solution content θ with depth on concentration-time curves, calculated with the finite difference method.

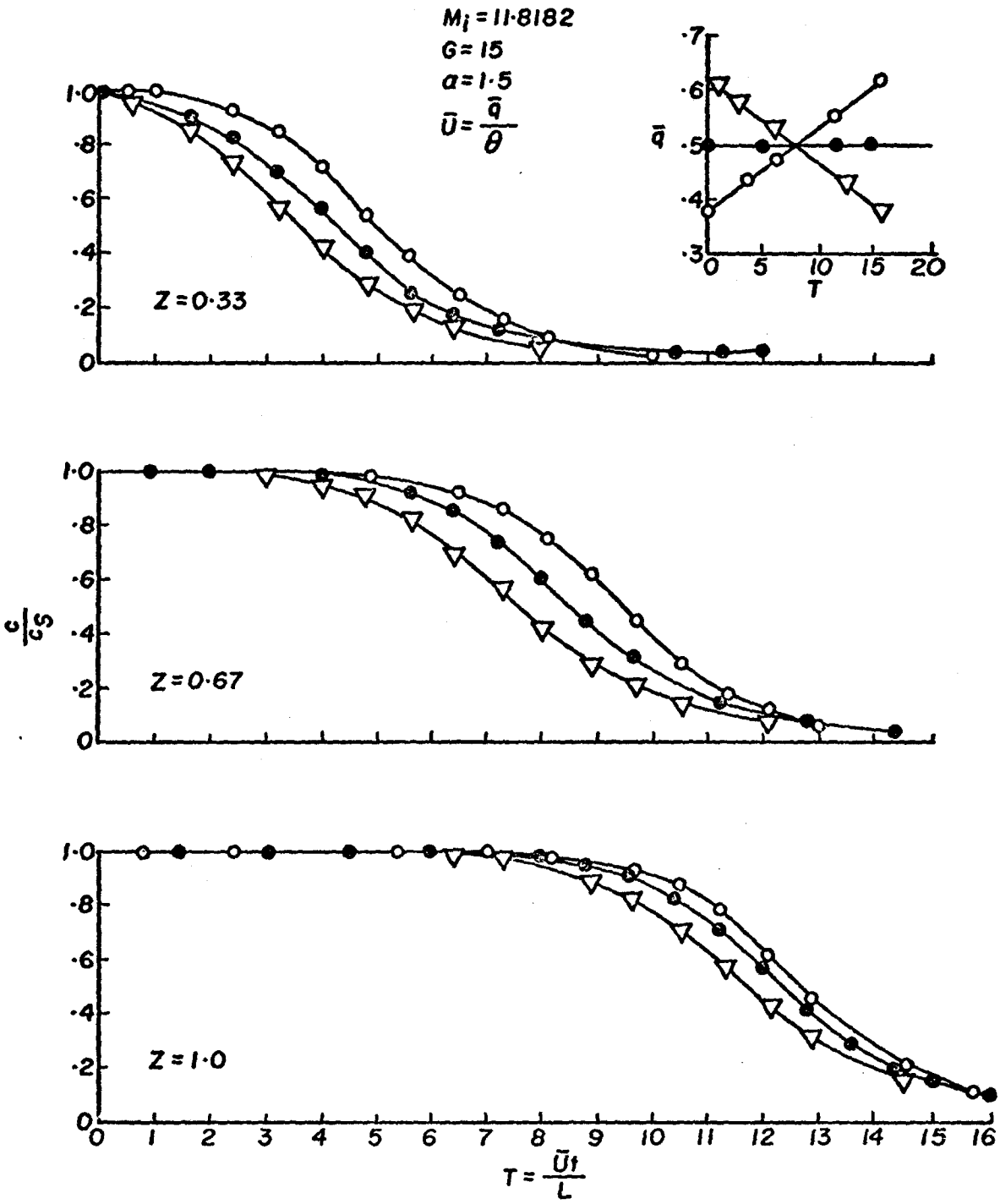

Fig. 17. The effect of a linear variation of the flow rate $\bar{q}$ with time on concentration-time curves calculated with the finite difference method.

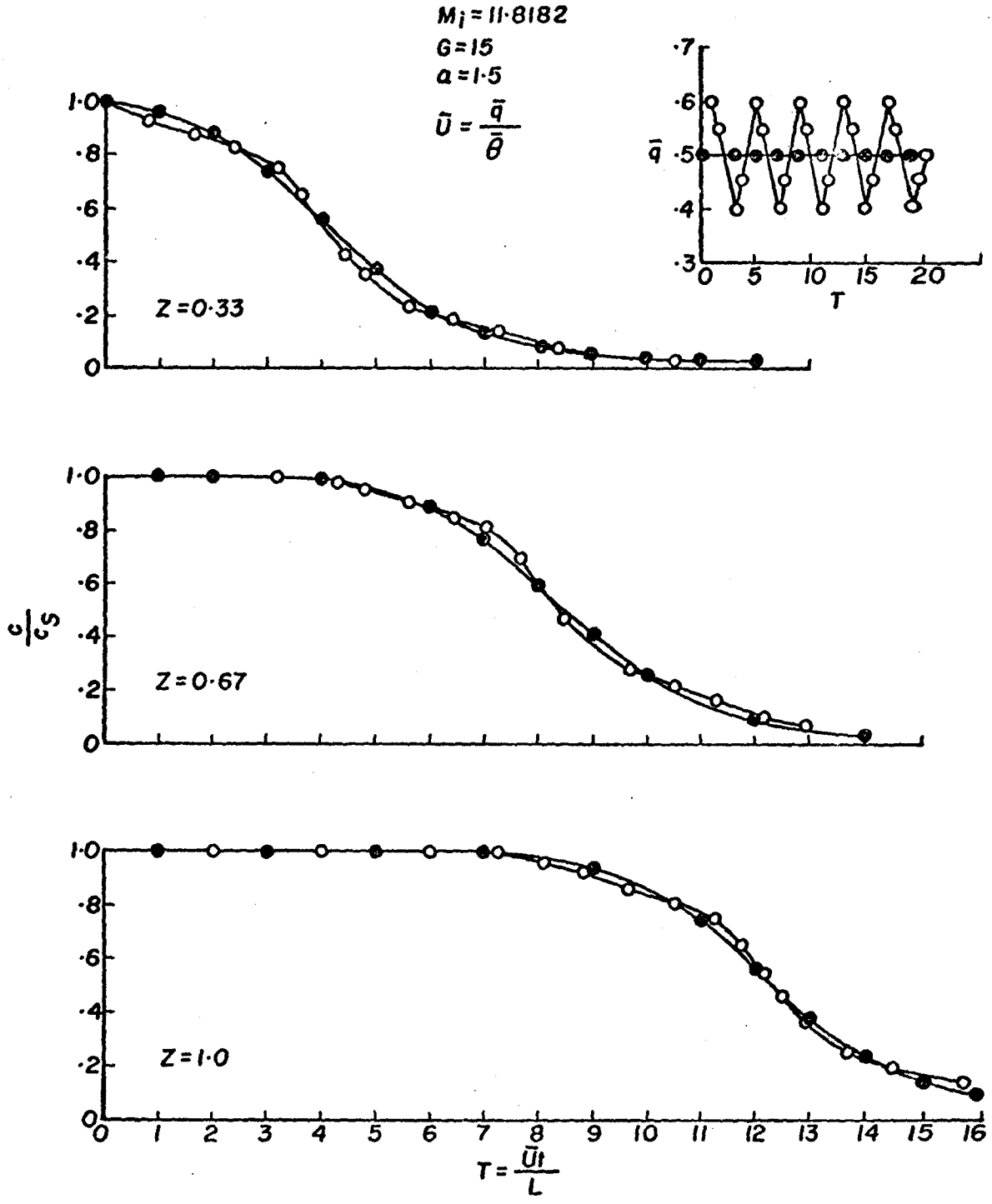

Fig. 18. The effect of a fluctuation of the flow rate $\bar{q}$ with time on concentration-time curves calculated with the finite difference method.

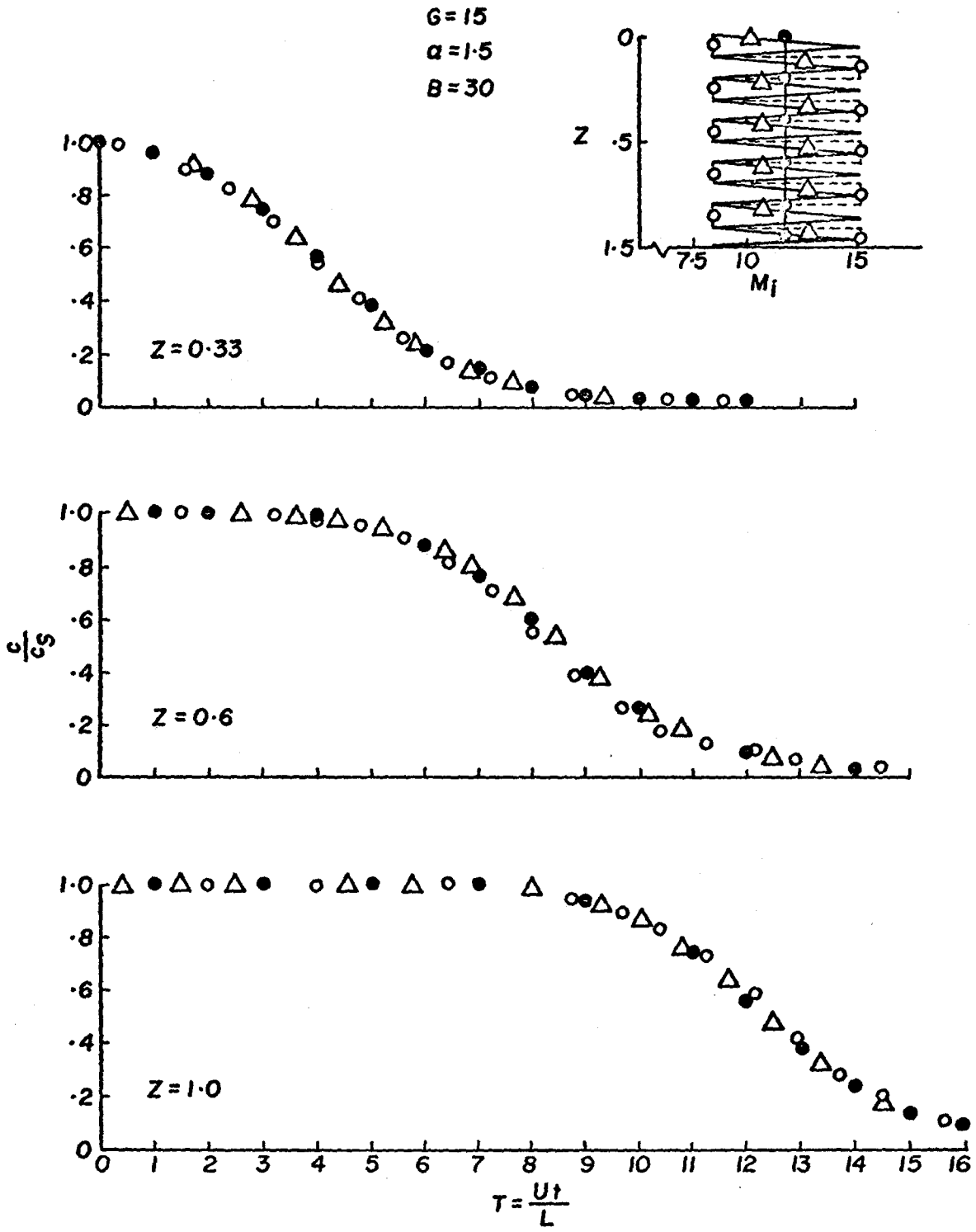

Fig. 19. The effect of a variation of M_i with depth on concentration-time curves calculated with the finite difference method.

found if the initial dimensionless mass of gypsum was calculated from $m_{i,t}/(\theta c_S)$, where $m_{i,t}$ is the total amount of gypsum material per unit volume of medium added to a column. The amount of pure gypsum that actually dissolved during an experiment was not equal to $m_{i,t}$, partly because of impurities in the gypsum material. Consequently M_i was estimated from mass balance principles using the measured concentration-time curve. This procedure, which is given in full detail in Glas (1976), required that the concentration measurements be continued until they had essentially reached zero. In some experiments this was not done, and an estimation of M_i was made using the available concentration-time data.

The Brenner number B for a given experiment was calculated from the seepage velocity, column length and a dispersion coefficient value obtained from the appropriate regression in Fig. 4.

Preliminary estimates of G and α were made by a graphical method which utilized the measured concentration-time curve in conjunction with the computed results of the kinetic model. For the details see Glas (1976). The preliminary estimates were then used to calculate the concentration-time curve. Upon comparison with the experimental data a decision was made whether or not further refinement of G and α was necessary. If so, an optimization procedure was utilized to improve the estimates of G and α.

The values of M_i, G and α obtained for each experiment are shown in Tables 8 and 9. The Brenner number values have already been given in Tables 6 and 7.

Graphical comparison of some results of the leaching studies with the mixing cell model and the kinetic model - The measured calcium concentration-time data from experiment 28 (black dots) are given in Fig.

Table 8. Values of M_i, G, α and F for the gypsum leaching studies performed in the sand.[1]

Exp.	Suction cup 1				Suction cup 2				Effluent			
No.	M_i	G	α	$Fx10^2$	M_i	G	α	$Fx10^2$	M_i	G	α	$Fx10^2$
1	9.4	30.0	0.5	0.28*	14.1	10.1	0.9	0.38				
2	11.7	142.1	1.4	0.30	11.8	16.1	0.4	0.42*	9.7	6.6	1.0	0.23
3	11.9	10.1	0.3	0.94	13.5	17.0	0.8	0.19	8.4	9.0	1.3	0.37*
3+									13.1	7.7	1.0	0.20*
4	7.5	27.3	0.9	0.34	8.7	10.3	1.3	0.05	10.2	4.7	1.0	0.13
5					15.5	12.3	1.2	0.81	16.1	4.5	1.2	0.37
6	5.3	15.0	0.8	0.43*	12.3	19.7	2.0	0.30	11.8	6.2	1.2	0.27
7	18.8	8.0	0.7	0.45*	18.1	3.9	0.6	0.18				
8	6.0	23.0	1.0	0.43*	8.8	11.3	2.1	0.36	7.8	7.5	1.2	0.22
9	6.8	16.6	0.9	0.12	6.8	17.0	1.6	0.16	10.0	4.9	0.5	0.27
10	8.8	2.7	2.6	0.21	6.5	2.8	2.3	0.32	7.9	3.2	1.2	1.88
11	5.3	14.0	1.3	0.14*	10.4	10.0	0.6	0.44*	10.5	11.4	1.2	0.13
12									9.6	15.0	1.3	0.18
13	7.0	8.0	1.8	0.18*	8.0	4.0	1.3	0.29*	10.1	3.6	1.0	0.26
14	16.6	2.8	1.2	0.76	10.6	1.6	1.5	0.60	16.3	1.0	1.4	0.69
15	8.5	5.0	2.8	0.05*	10.2	2.5	1.2	0.35*	13.3	4.0	1.2	0.29*
17	7.1	4.0	0.7	0.08*	8.7	5.0	1.3	0.16*	9.0	3.5	1.1	0.10
17+									8.8	3.1	1.2	0.20
18					1.2	2.0	1.5	0.61	3.6	1.5	1.5	0.71
19	5.5	2.3	1.2	0.36	6.8	2.8	1.1	0.10	5.8	1.7	0.9	0.41
20	12.4	4.5	2.2	0.12*	11.1	3.0	1.6	0.22*	8.9	2.0	1.5	0.29*
20+									11.4	2.5	1.5	0.24*
21	10.0	2.2	1.1	0.05	8.7	2.1	1.2	0.09	11.9	1.9	1.4	0.17
22					5.0	1.0	1.8	0.31*				
23	5.5	17.6	1.3	0.41	7.4	25.0	1.2	0.24	9.4	4.1	1.0	0.15
24	5.3	24.0	1.0	0.47*	5.7	26.4	0.8	0.86	5.3	30.0	1.0	0.42*
24+									5.1	18.6	0.8	0.86
25	3.0	15.0	0.8	0.48*	4.5	19.0	1.6	0.40*	5.9	5.0	0.9	0.18*
26	15.8	14.0	0.9	0.34	14.7	8.1	1.0	0.07	11.6	6.2	1.2	0.19
27	18.0	20.5	0.8	1.08	14.1	35.0	0.75	0.07	12.0	14.0	1.2	0.08*
27+									11.6	30.0	1.3	0.28*

* G, α and F obtained from the graphical procedure.

+Data from suction cup located directly above the bottom of the column.

Table 9. Values of M_i, G, α and F for the gypsum leaching studies performed in the clay.

Exp.	Suction cup 1				Suction cup 2				Effluent			
No.	M_i	G	α	$Fx10^2$	M_i	G	α	$Fx10^2$	M_i	G	α	$Fx10^2$
28	4.2	20.9	1.9	0.21	3.9	26.1	2.1	0.30				
29	8.3	39.0	0.8	0.24	8.3	11.5	0.8	0.21	7.5	7.2	0.9	0.60
30	14.6	30.7	2.4	0.46	9.7	10.6	1.9	0.29	10.2	10.0	1.4	0.32
31	7.2	12.5	0.6	0.36*								
32	1.7	15.0	0.8	0.23*	2.6	6.1	0.4	0.48	3.1	5.3	1.4	0.18
32+									2.7	4.3	1.2	0.25
33	8.4	17.6	0.7	0.21	10.0	6.4	0.8	1.44	8.8	5.7	0.9	0.43
34	3.0	24.0	1.9	0.05*	14.9	8.1	1.3	0.72	7.9	2.5	1.2	0.37*
35	2.8	28.7	2.8	0.37*	3.2	17.5	1.5	0.20	3.4	16.0	1.5	0.05
36	9.2	46.7	0.6	0.09	11.6	12.7	0.9	0.40	9.9	4.5	1.2	0.20
36+									9.9	19.0	1.0	0.14
37	2.6	14.0	0.6	0.28*	2.8	5.6	0.4	0.36	2.4	4.0	0.8	0.21
38	2.4	15.0	0.8	0.18*	4.5	13.1	0.7	0.17	3.6	4.9	1.1	0.11
39	4.0	15.0	2.2	0.22*	3.9	24.2	2.0	0.22				
40					9.0	2.5	1.5	0.27	10.9	1.9	2.0	1.05
40+									10.1	2.0	1.5	0.83*
41					10.2	7.5	2.1	0.37*	7.6	11.4	1.7	0.23
42	6.6	4.2	1.2	0.55	4.1	4.2	1.5	0.34	4.1	2.5	1.1	0.36*
43	2.6	8.0	2.6	0.47*	3.0	2.5	1.2	0.29*	3.5	4.0	1.2	0.44*
44					4.3	5.3	1.4	0.28*	3.7	5.0	1.0	0.53
45	1.5	0.9	1.2	0.43	2.3	1.0	1.3	0.18	2.0	1.5	0.7	0.13
46	4.5	3.0	2.5	0.33*	4.5	3.4	2.0	0.22	5.2	3.0	1.8	0.22
47	4.9	9.5	1.9	0.40*	4.3	3.3	1.5	1.13	6.0	3.6	1.5	0.16
47+									5.4	4.0	1.6	0.13*
48	6.9	117.2	1.0	0.24	6.5	6.9	1.0	0.19	4.7	5.1	1.1	0.12
49	5.0	12.5	0.8	0.17*	5.7	10.0	1.1	0.18	5.0	4.7	1.1	0.23
50	17.6	45.0	1.5	1.31	17.0	40.2	1.1	0.45	12.3	6.6	1.0	0.29

*G, α and F obtained from the graphical procedure

+Data from suction cup located directly above the bottom of the column.

20. The prediction of the mixing cell model (step-type curve) and the results of fitting the kinetic model to the experimental data are also given. The mixing cell model was not capable of representing the experimental data. Good agreement between the data and the kinetic model was obtained even with the preliminary estimate of G and α (dashed curve), and some improvement was attained by optimization (solid curve). Note that different values of M_i G and α were obtained for the two sampling depths.

Figure 21 shows the measured concentration-time data of experiment 20 compared with the mixing cell model and the kinetic model. Again the mixing cell model is incapable of representing the results. With the kinetic model it is possible to describe the experimental results, but the parameters G, α and M_i vary with position.

Another example of comparison between the experimental data and the two models is shown in Fig. 22 for the data of experiment 36. In this case G decreased with position while α increased.

Behavior of the parameters G, α, M_i and k_i - The reaction rate parameter G for each sampling position is plotted against particle size class in Fig. 23. The data are very scattered, but the parameter tends to decrease with increasing particle size, and thus with decreasing surface area of the material. Several authors have suggested or noticed a possible relation of this kind between the surface area and the reaction rate parameter. The average value of G for each particle size class tends to decrease with increasing depth from the top of the column, except for the two largest size classes where G remains approximately constant. A possible explanation for this decrease of G with increasing depth may be the formation of less soluble coatings on the

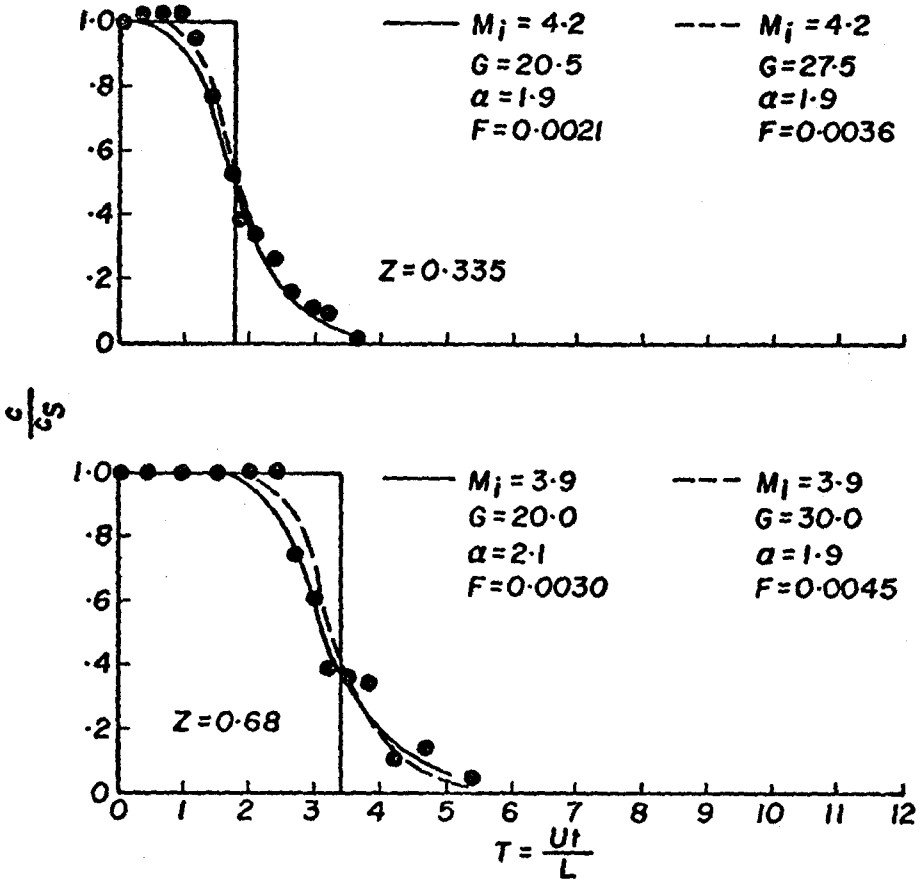

Fig. 20. Comparison between the measured calcium concentrations from experiment 28 (black dots), results from the mixing cell model (solid straight lines) and results from the kinetic model based on parameters from the graphical procedure (dashed curves) and from the optimization procedure (solid curves).

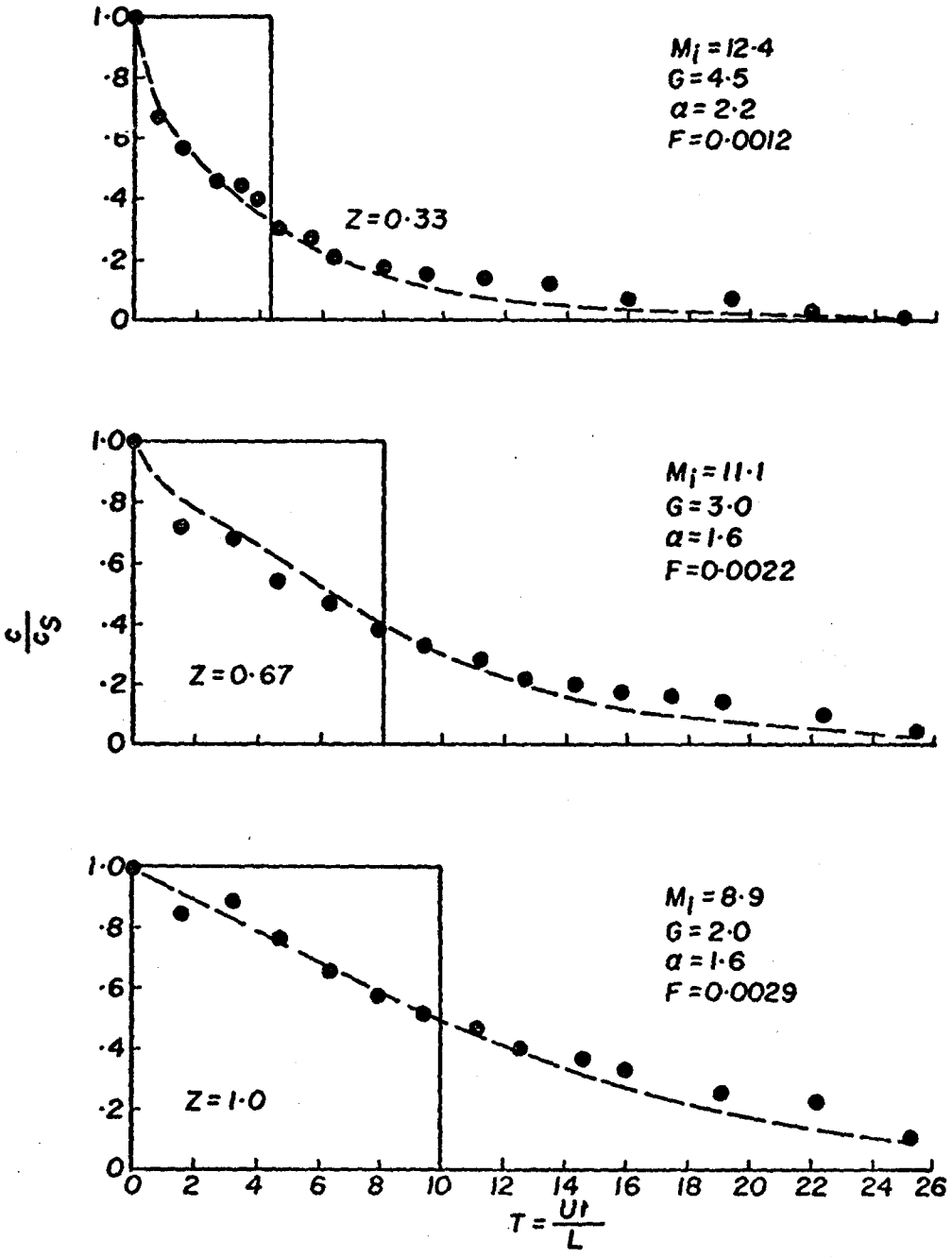

Fig. 21. Comparison between the measured calcium concentrations from experiment 20 (black dots), results from the mixing cell model (solid straight lines) and results from the kinetic model based on parameters from the graphical procedure (dashed curves).

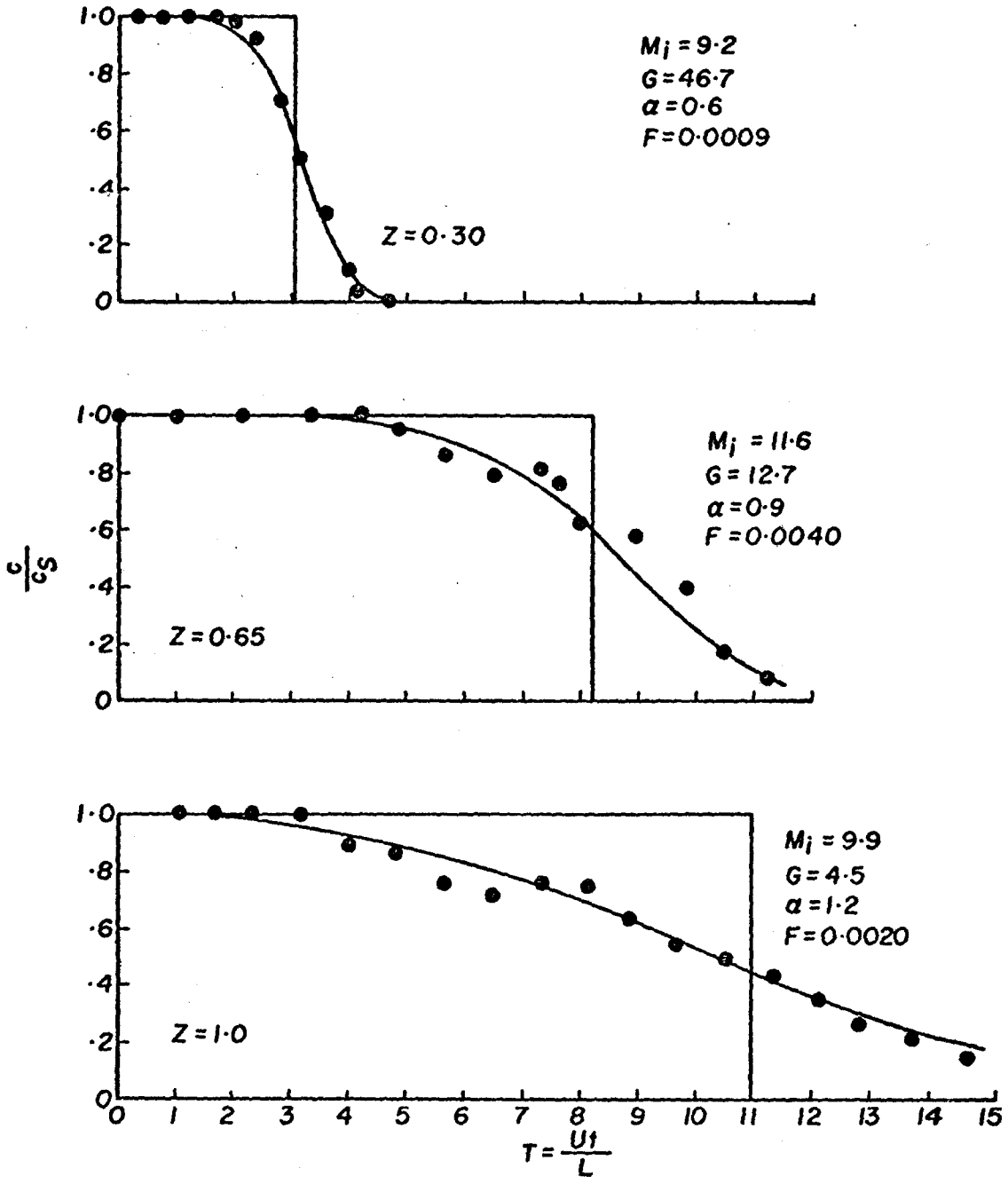

Fig. 22. Comparison between the measured calcium concentrations from experiment 36 (black dots), results from the mixing cell model (solid straight lines) and results from the kinetic model based on parameters from the optimization procedure (solid curves).

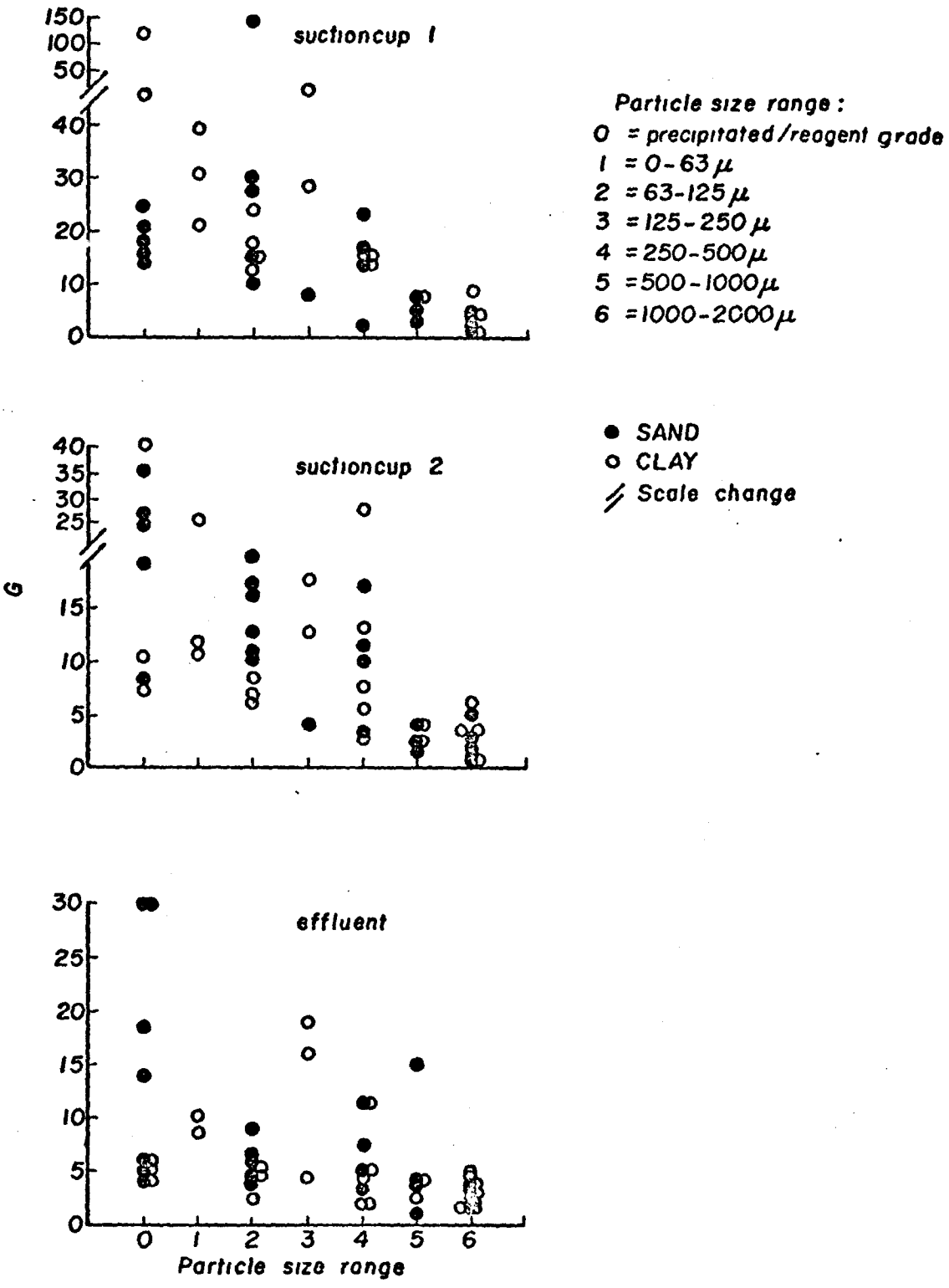

Fig. 23. Plots of the dimensionless reaction rate parameter G against particle size of the gypsum material in the sand (black dots) and in the clay (open circles).

gypsum particles after they have been present in the soil column for a period of time. Barrows et al. (1966) found that surface coatings formed on limestone particles shortly after they were placed in soil due to the combined processes of weathering and recrystallization of calcite and adsorption or precipitation of phosphates from the soil. In the gypsum leaching experiments, particles located at a greater depth were in contact with the soil for a longer time, and were subjected to the possible formation of surface coatings for a longer time. If such a process were operative we would expect the reaction rate parameter to decrease with depth. However, whether this mechanism is applicable is somewhat speculative and further study is required.

No systematic differences were found between the values of G for the sand and the clay, nor was there any systematic difference between G values for saturated or unsaturated conditions.

Figure 24 shows the reaction rate parameter G plotted against seepage velocity. There seems to be some tendency for G to decrease with increasing U, although the trend is poorly defined. The physical reaction rate parameter, $k_i = G\,U/L$, showed no discernible trend with seepage velocity. Values of k_i were on the order of $1\ hr^{-1}$, and decreased with increasing depth in accordance with the same trend in G.

The parameter α is plotted against particle size in Fig. 25. No systematic trends with respect to particle size, or sampling depth can be noticed. There does not seem to be any effect of seepage velocity upon the parameter α (see Tables 6, 7, 8 and 9). It is concluded from these observations that α is a purely empirical parameter that varies from experiment to experiment for reasons that cannot be adequately explained at this time. The average value of α for the sand was about 1.2, that for the clay was about 1.4.

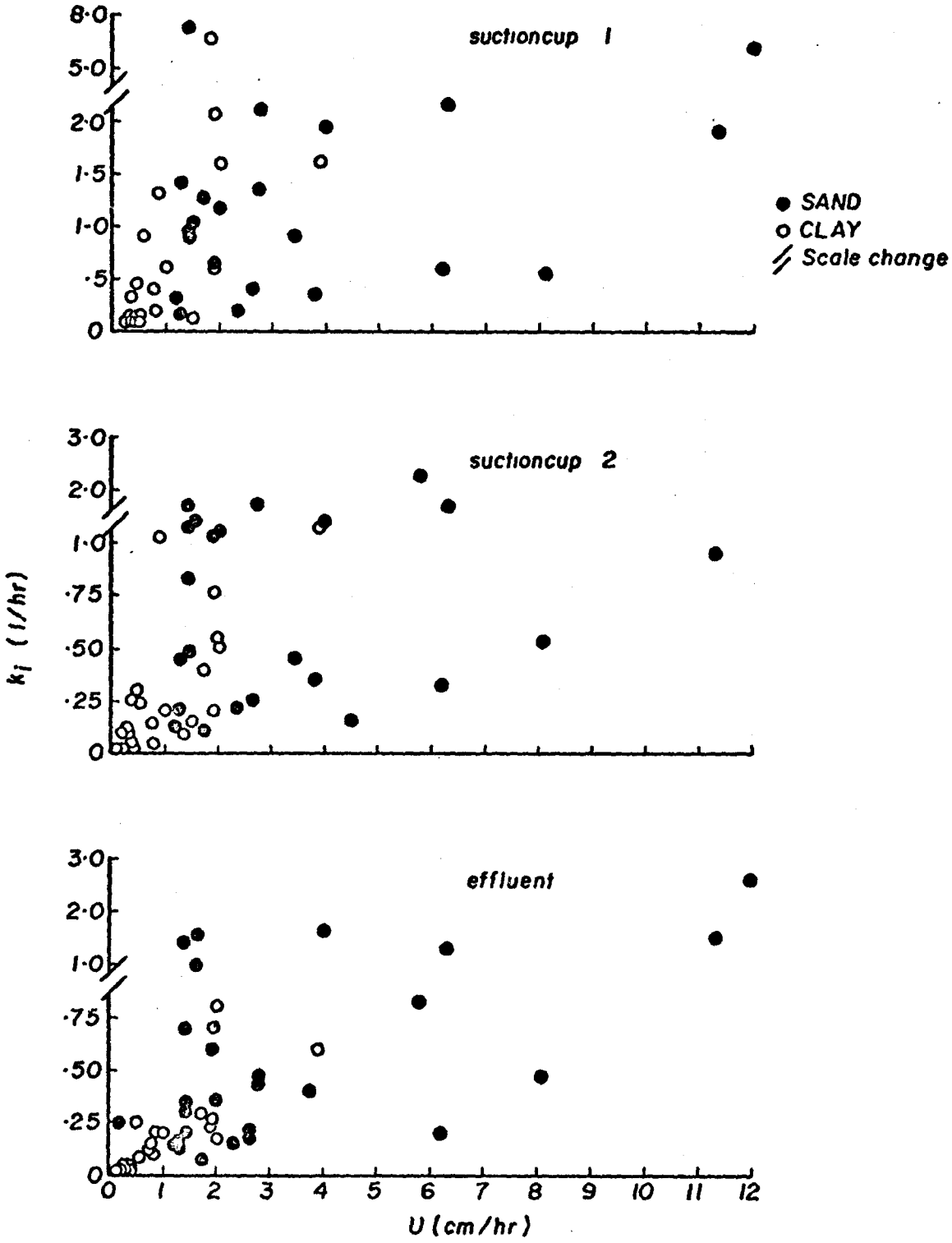

Fig. 24. Plots of the reaction rate parameter k_i against the seepage velocity U in the sand (black dots) and in the clay (open circles).

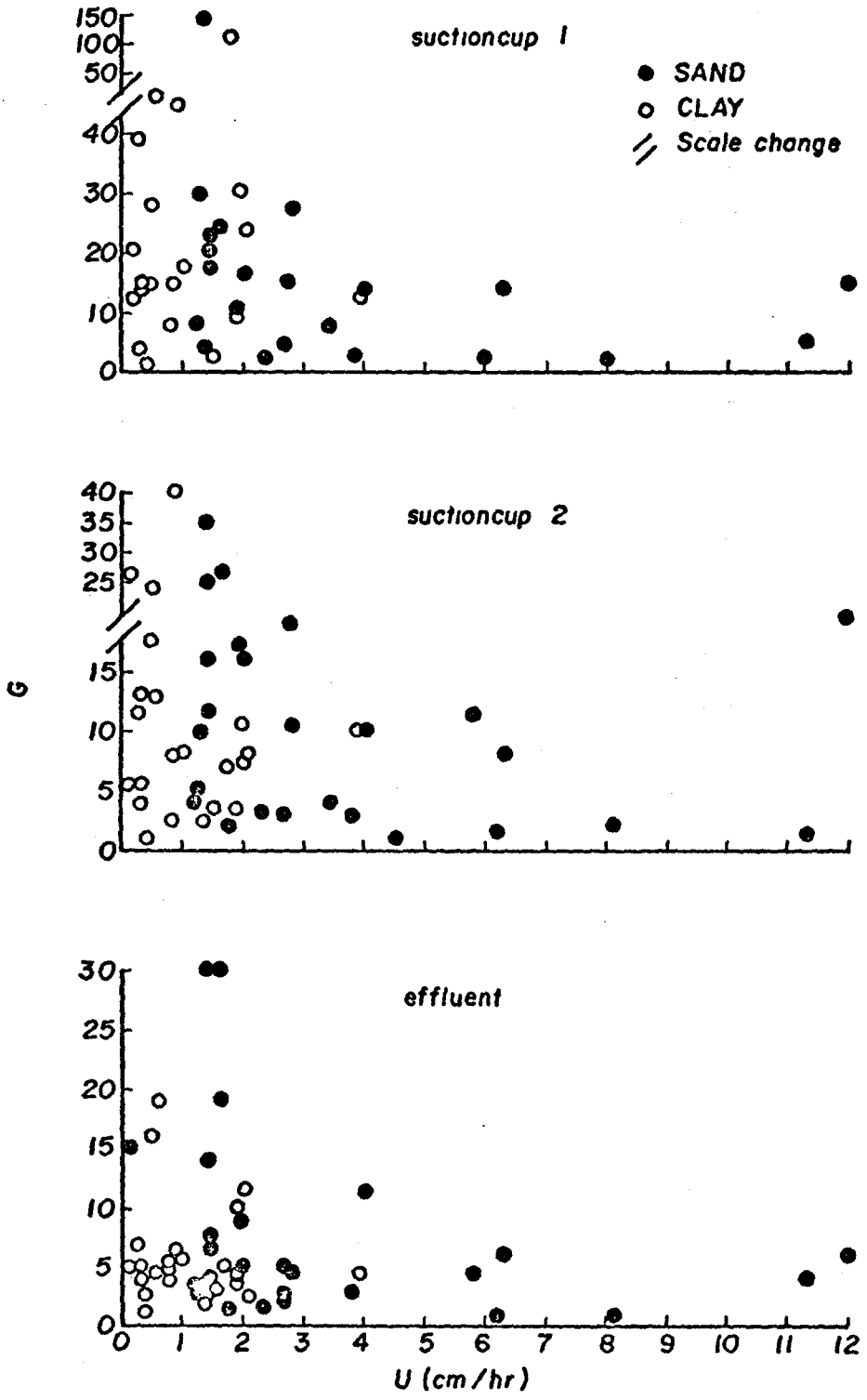

Fig. 25. Plots of the dimensionless reaction rate parameter G against the seepage velocity U in the sand (black dots) and in the clay (open circles).

Different values of the parameters G, M_i and α were obtained from the concentration-time curves at each sampling depth in a given experiment. The process of estimating the parameters utilized solutions to the kinetic model (Eqs. (43) and (44)) in which the parameters were assumed independent of position. Consequently the parameter values obtained at each position are not the "actual" values of G, M_i and α applicable in a given section of the column, but are some kind of average values, which are related to the actual space dependent parameters in an unknown way.

The effect of step-wise variations with depth of the parameters G, α and M_i on the concentration-time curves was explored using the kinetic model. The results of these calculations are shown in Figs. 26, 27 and 28. The magnitude of the imposed variations in the parameters are comparable to those observed in the results from the leaching experiments. All curves calculated for a variable parameter were compared with curves obtained for a constant average value of the parameter.

The results (Fig. 26) for a variable M_i differ significantly from those for a constant M_i at positions $z=0.32$ and $z=0.68$, but the difference is small at $z=1.0$. The effect of a variation in G (Fig. 27) is especially pronounced in those regions where G is smaller than the average. The spatial variation of α had little effect on the concentration-time curves (Fig. 28).

While it would be possible to formulate a kinetic model in which the parameters were functions of position, it would not be feasible to fit the results of such a model to experimental data by optimization since the number of parameters to be found by optimization is proportional to the number of different layers which are considered to be present and the required computer time would become too great.

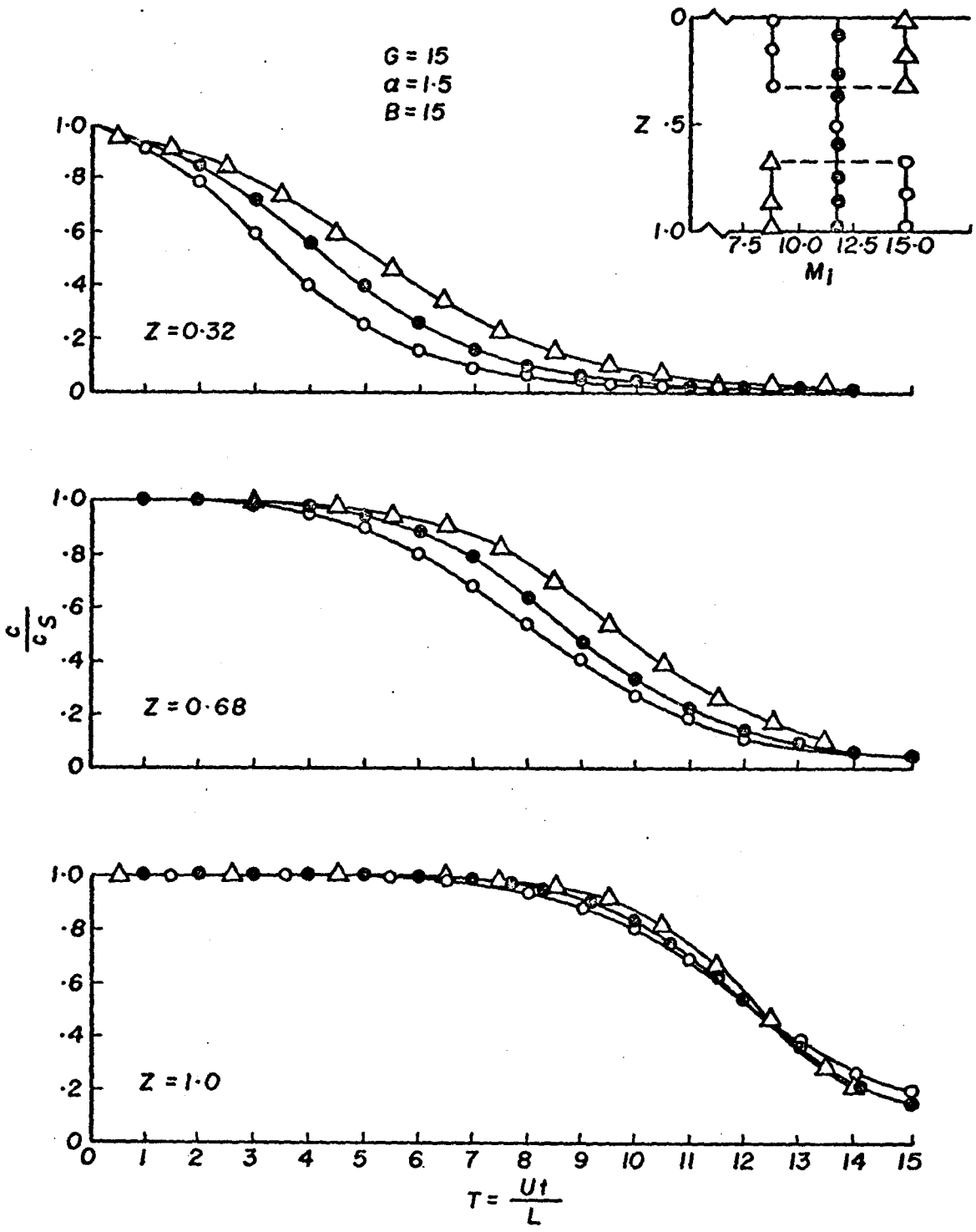

Fig. 26. The effect of a stepwise variation of the parameter M_i with depth in the kinetic model.

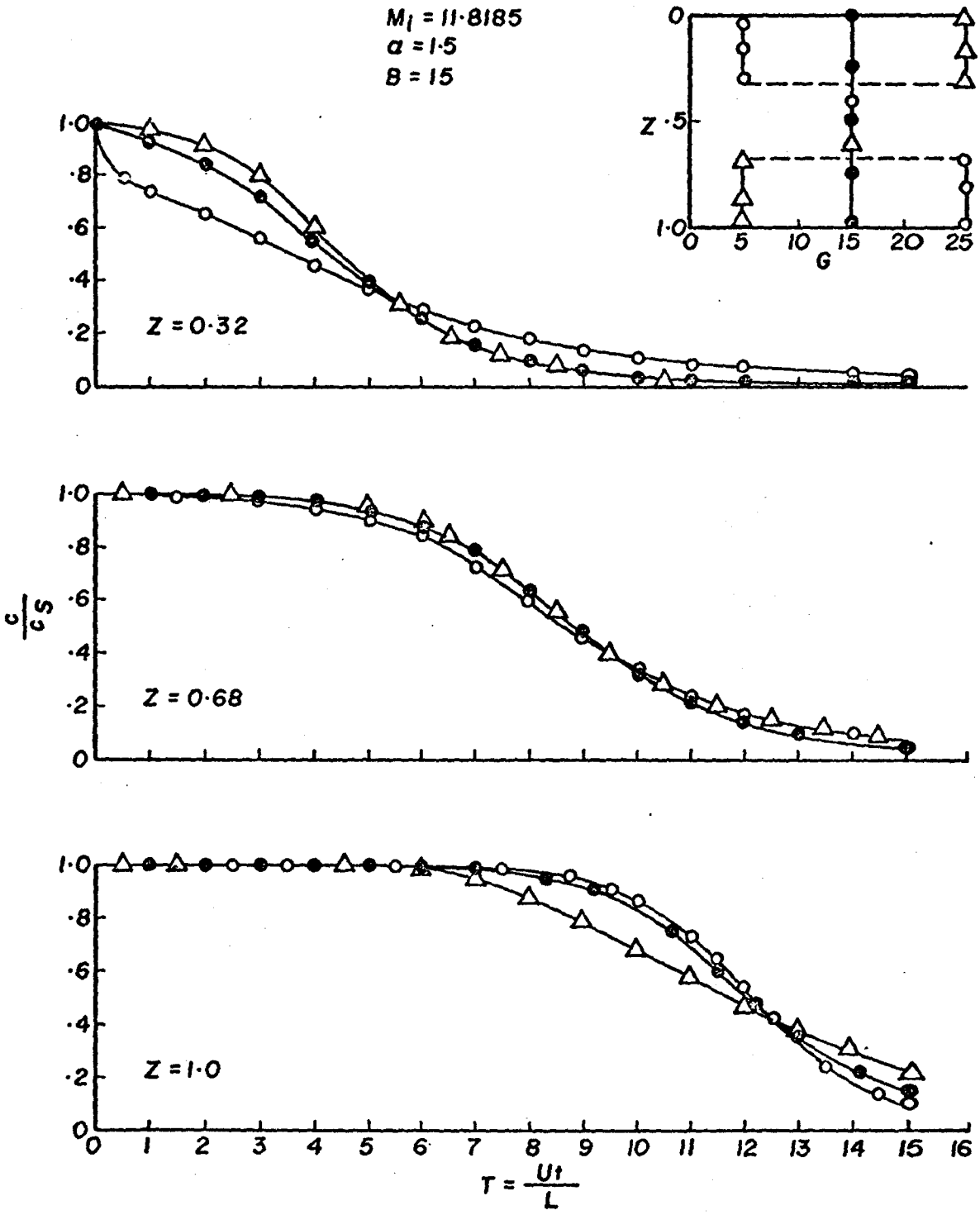

Fig. 27. The effect of a stepwise variation of the parameter G with depth in the kinetic model.

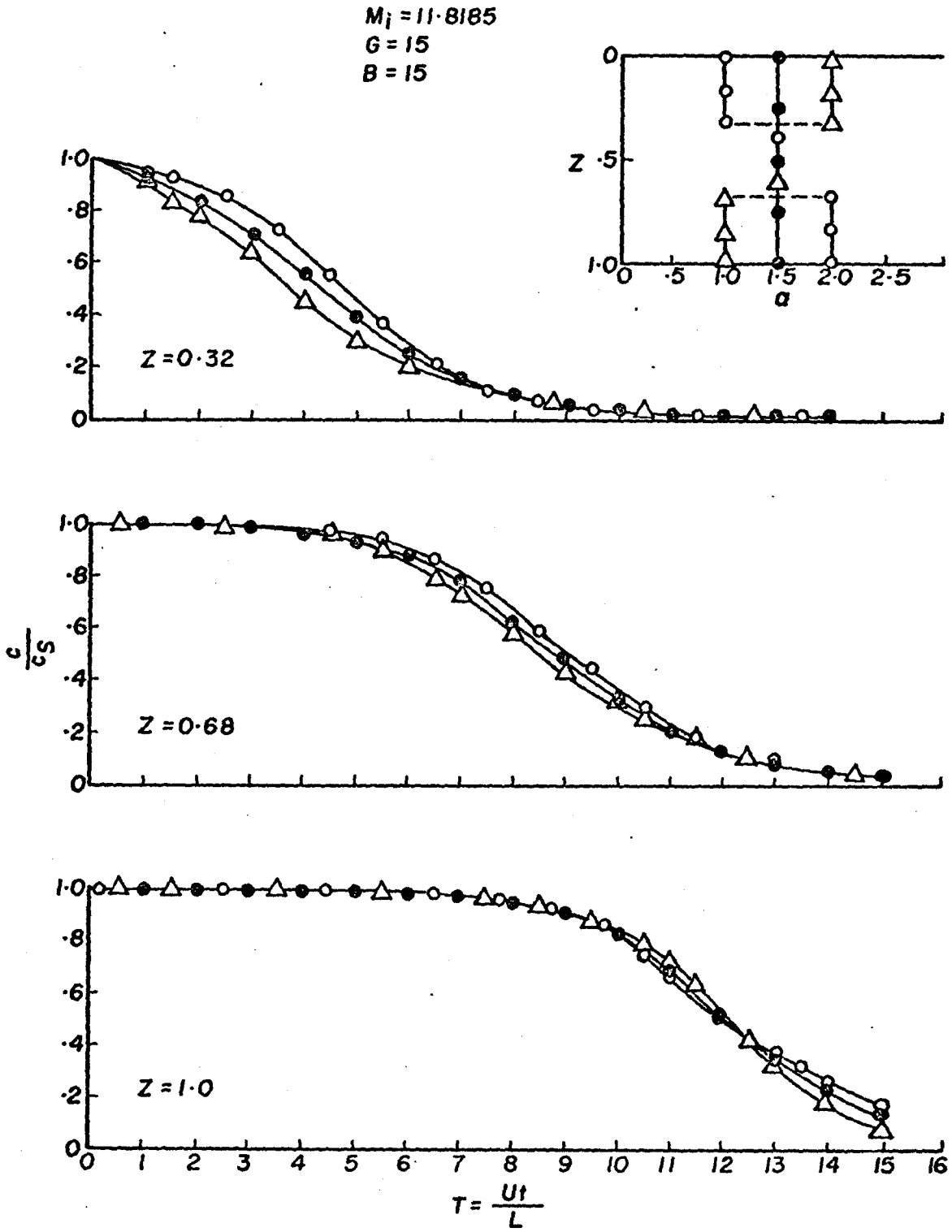

Fig. 28. The effect of a stepwise variation of the parameter α with depth in the kinetic model.

The kinetic source term model used in this study is of the form:

$$\frac{dm}{dt} = K_1(c-c_S) \tag{53}$$

where $K_1 = k_i(m/m_i)^{\alpha}\theta$ is the effective dissolution rate parameter.

A possible approach to a theory from which K_1 could be calculated is based on the theory described by Millington and Powrie (1968). These authors calculated the dissolution rate of a single particle from:

$$\frac{d\bar{m}}{dt} = k_m \pi d^2 \frac{\bar{c}-c_S}{c_S-\bar{1}} \tag{54}$$

where k_m was calculated from:

$$k_m = \frac{\rho_w D}{d}\left[2 + 0.6\, d^{1/2}\left(\frac{U\rho_w}{\eta}\right)\left(\frac{\eta}{\rho_w D}\right)^{1/3}\right] \quad . \tag{55}$$

In the above d is the particle diameter, ρ_w is the density of solution, D is the molecular diffusion coefficient, U is the seepage velocity and η is the fluid viscosity. If we assume that the source function in the kinetic model, is given by $N\, d\bar{m}/dt$, where N is the number of equal-sized particles per unit volume of porous mdeium then we can write:

$$G_i = [f_1 d + f_2 d^{3/2}](c-c_S) \tag{56}$$

where f_1 is a constant and f_2 is a function of seepage velocity. Assuming that the particles are spherical, $d = [(6m)/(\rho N\pi)]^{1/3}$ and Eq. (56) can be written

$$G_i = [F_1 m^{1/3} + F_2 m^{2/3}](c-c_S) \quad . \tag{57}$$

From this the effective dissolution rate parameter is found to be

$$K_2 = (F_1 m^{1/3} + F_2 m^{2/3}) \quad . \tag{58}$$

Comparison of K_2 with K_1 indicates that K_2 will not describe the dissolution in the present experiments. The parameter K_1 contains a term m^{α} where α is on the order of 1.2 to 1.4 . The parameter K_2 shows a more complex dependence on m but it does not appear to be as strongly dependent on m as K_1 . From this it is concluded that a dissolution rate based on the Millington-Powrie theory does not describe the leaching of gypsum in the present experiments.

Effect of seepage velocity variation - The flow rate of the solution phase was delibrately varied with time in experiments 37 and 16. In experiment 37, the flow rate was changed periodically with time in such a way that it was either approximately 0.3 cm/hr or zero for periods of time of about 12 hours. The results from this experiment are shown in Fig. 29. In experiment 16 the flow rate was kept constant at about 0.6 cm/hr except during the time period between 75 and 200 hours from the start of the experiment when the flow rate was zero (Fig. 30).

The increases in calcium concentration that occurred during periods of zero flow in both experiments is another indication of the kinetic nature of the dissolution process. If the process were controlled by the solubility product relationship, the concentration in the solution phase would not have been affected by the variation in flow rate.

By assuming that the solution phase flow took place at a constant flow of 0.15 cm/hr in experiment 37, which is the integrated mean of the varying flow rate, values of G and α were estimated. These values of G and α are listed in Table 9 and the corresponding concentration-time curves are shown as solid lines in Fig. 29. A reasonable fit to an "average" concentration-time curve was obtained in this manner.

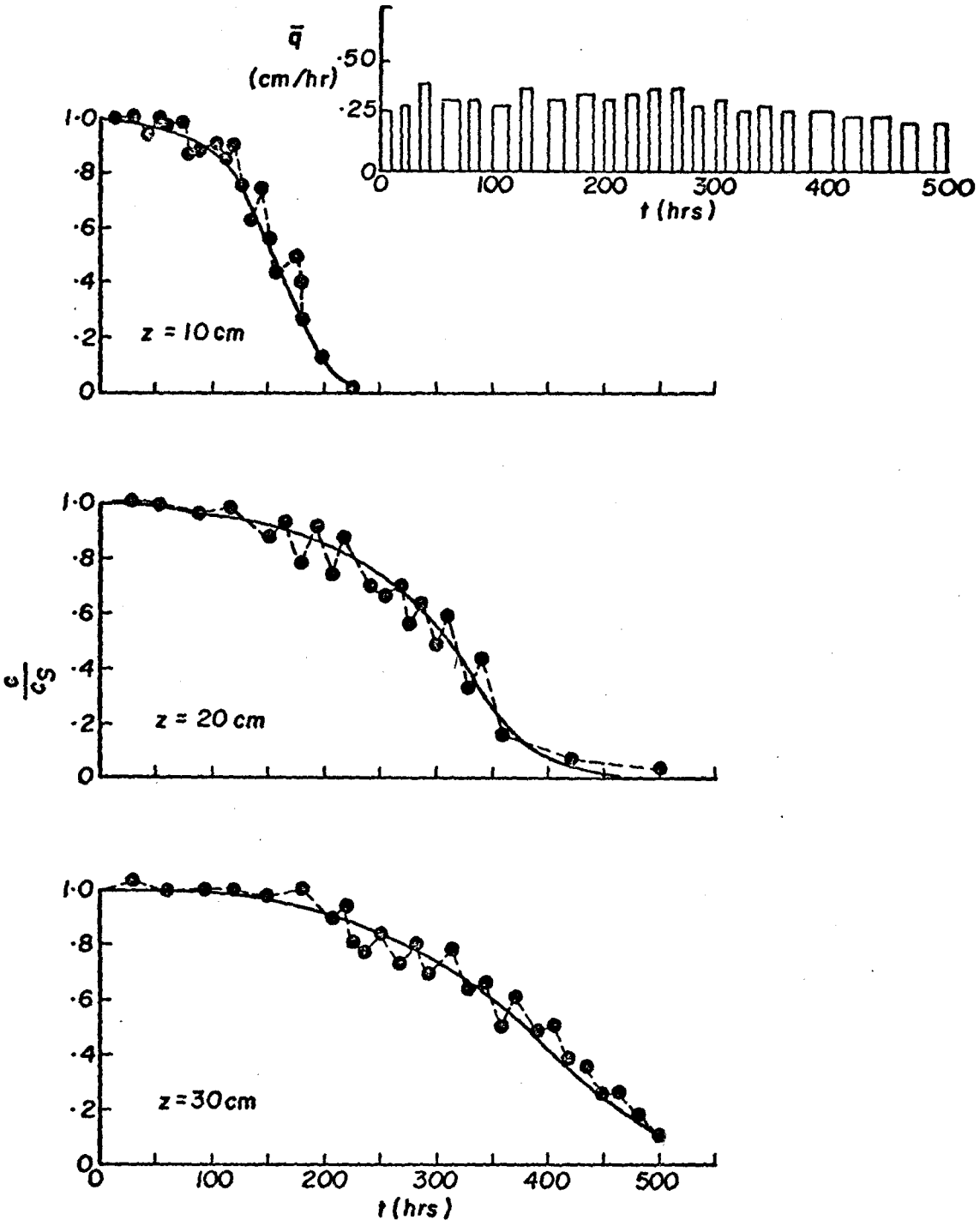

Fig. 29. Comparison between the measured dimensionless calcium concentration in experiment 37 (black dots) and results from the kinetic model (solid lines).

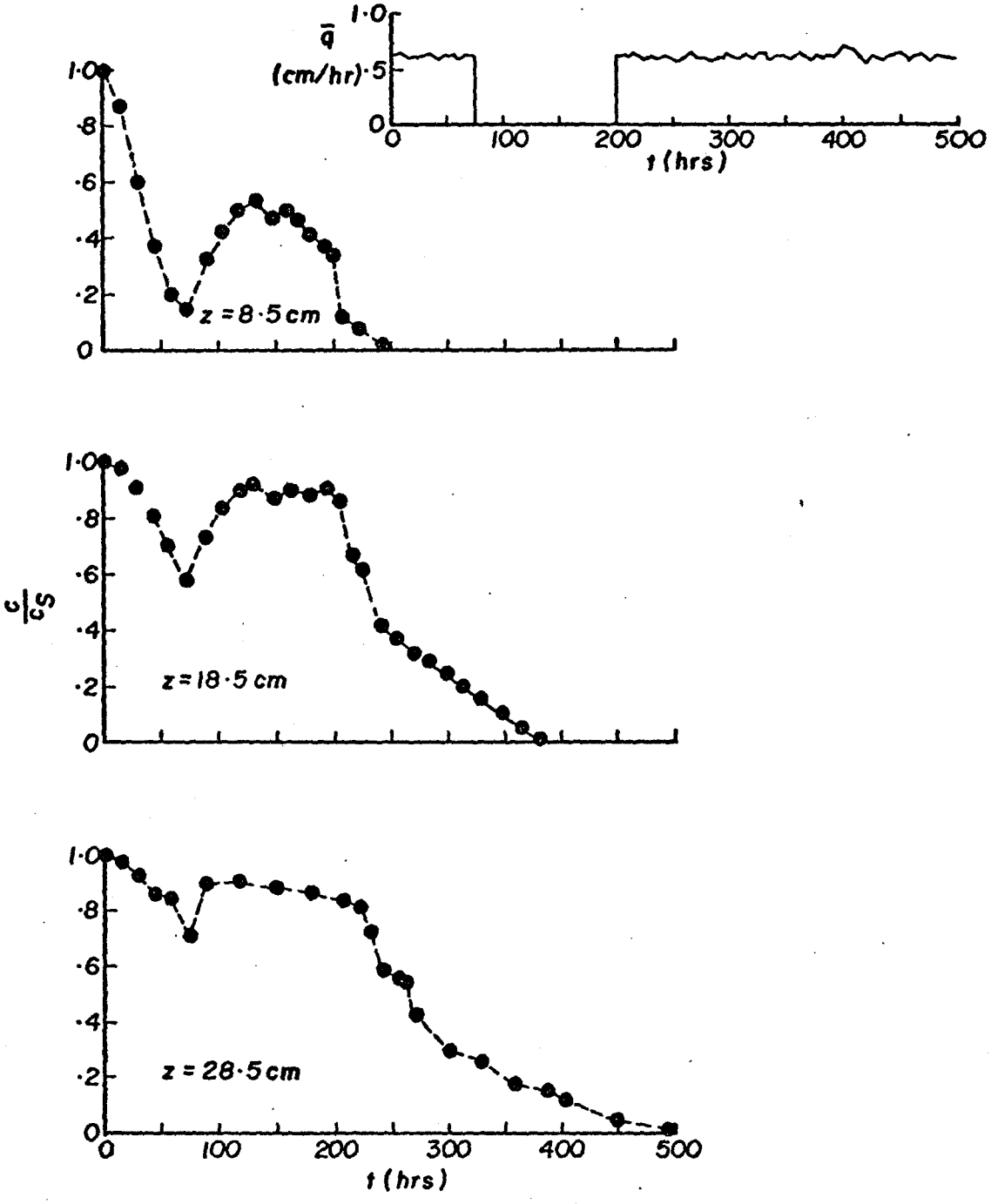

Fig. 30. Plots of the measured dimensionless calcium concentration against physical time (hours) for experiment 16 (black dots).

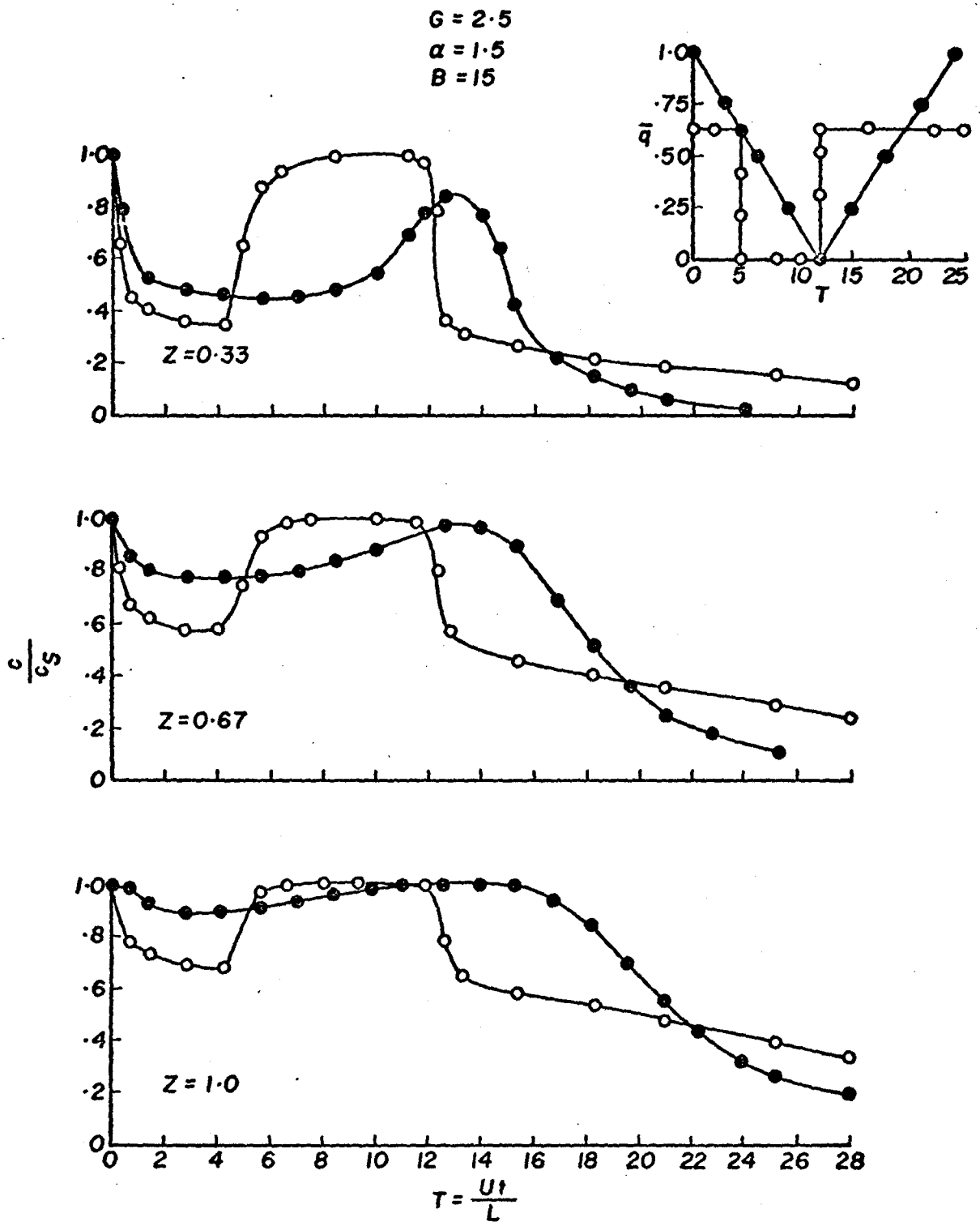

Fig. 31. Concentration-time curves calculated with the finite difference method for a Darcy velocity $\bar{q}$ varying with time.

Concentration-time curves for a Darcy velocity varying linearly and step-wise with time were calculated from the kinetic model using the finite difference method of solution (Fig. 31). The step-wise flow rate variation in this simulation is similar to that imposed in experiment 16. A qualitative similarity can be seen between the simulated results and those from experiment 16.

CHAPTER IV

CONCLUSIONS

The concentration-time curves obtained from gypsum leaching experiments were compared with two models, a mixing cell model based on equilibrium principles, and a kinetic transport model based on the dispersion-convection equation in combination with a kinetic expression for the source term which represented the dissolution of solid phase gypsum. Under the conditions of the leaching experiments (gypsum particle sizes ranging from less than 63μ to 2000μ ; two soils, a sand and a clay; seepage velocities from 0.1 cm/hr to 12 cm/hr; saturated and unsaturated soils) the mixing cell model could not represent the observed concentration-time curves and a kinetic source term description was required.

The kinetic source term representation used in this study was:

$$G_i = -k_i\left(\frac{m}{m_i}\right)^{\alpha}\theta(c-c_s)$$

where G_i is the mass of gypsum dissolved per unit of time and per unit volume of soil, and k_i , m_i and α are parameters. By adjustment of the three parameters the observed concentration-time curves could be satisfactorily fitted with a solution of the dispersion-convection equation which included the above source term representation.

A dimensionless reaction rate parameter, $G = (k_i L)/U$, tended to decrease with increasing gypsum particle size, and with increasing seepage velocity, although the trends were poorly defined. The parameter m_i could not be determined from the amount of added gypsum material partly because of impurities in the material, but also because of some other reason(s). Speculative possibilities as the formation of coatings on the gypsum particles and the location of some of the particles in

micro-zones that are relatively inaccessible to convective flow of the solution phase. The parameter α seems to have no physical basis and remains an empirical parameter.

While it was clear that a kinetic source term representation was necessary to describe the dissolution process, the problem of a source term model is still not satisfactorily solved. A model such as the one used in this study, which contains one or more empirical parameters, requires that those parameters be determined using the very data that one desires to predict. Such a situation is not entirely unsatisfactory if the empirical parameters can be measured in a reproducable manner and established as properties of the soil-water-gypsum system. Whether this in fact can be done is as yet uncertain. A more satisfactory source term model would be one built upon a theory of the dissolution process, with less empiricism in it, and would allow a better possibility of prediction of the leaching process. An example of this kind of approach is that used by Millington and Powrie (1968). However, from the brief examination of their theory made to date it does not appear that their theory will describe the dissolution process. Some further study of this approach seems warranted, however.

BIBLIOGRAPHY

Adams, F. 1972. Ionic concentrations and activities in soil solutions. Soil Sci. Soc. Amer. Proc. 35:420-426.

Barrows, H. L., Simpson, E. C. and Tu, H. Y. 1966. Formation of surface coatings on limestone particles in soils. Soil Sci. Soc. Amer. Proc. 30:317-320.

Barton, A. F. M. and Wilde, N. M. 1971. Dissolution rates of polycrystalline samples of gypsum and orthorhombic forms of calcium sulfate by a rotating disc method. Trans. Fara. Soc. 67:3590-3597.

Bear, F. E. and Allen, L. 1932. Relation between fineness of limestone particles and their rates of solution. Ind. Eng. Chem. 24:998-1001.

Bear, J. 1972. Dynamics of fluids in porous media. Elsevier, New York.

Bear, J. and Todd, D. K. 1960. The transition zone between fresh and salt waters in coastal aquifers. Univ. of Calif., Water Res. Center Contrib. No. 29.

Bennett, A. C. and Adams, F. 1972. Solubility and solubility product of gypsum in soil solutions and other aqueous solutions. Soil Sci. Soc. Amer. Proc. 36:288-291.

Berry, L. G. and Mason, B. 1959. Mineralogy: concepts, description, determinations. Freeman, San Francisco.

Bird, R. B., Stewart, W. E. and Lightfoot, E. N. 1960. Transport phenomena. Wiley, New York.

Boast, C. W. 1973. Modeling the movement of chemicals in soils by water. Soil Sci. 115:224-230.

Brenner, H. 1962. The diffusion model of longitudinal mixing in beds of finite length. Numerical values. Ind. Engr. Sci. 17:229-243.

Bresler, E. 1973. Simultaneous transport of solutes and water under transient unsaturated flow conditions. Water Resources Res. 9:975-986.

Deemter, J. J. van, Zuiderweg, F. J. and Klinkenberg, A. 1956. Longitudinal diffusion and resistance to mass transfer as causes of non-ideality in chromatography. Chem. Eng. Sci. 5:271-289.

Dutt, G. R. and Tanji, K. K. 1962. Predicting concentrations of solutes in water percolated through a column of soil. J. Geophys. Res. 67:3437-3493.

Dutt, G. R., Shaffer, M. J. and Moore, W. J. 1972. Computer simulation model of dynamic bio-physicochemical processes in soils. Agricultural Experiment Station, Univ. of Arizona, Tucson, Ariz. Technical Bulletin 196.

Elphick, B. L. 1955. Studies in use of agricultural limestone: II. Solubility of limestone in acid soil as influenced by particle size. New Zealand J. Sci. and Techn. 37A:156-173.

Frissel, M. J. and Poelstra, P. 1967. Chromatographic transport through soils I. Theoretical evaluations. Plant and Soil 26:285-302.

Gerson, N. D. and Nir, A. 1969. Effects of boundary conditions of models on tracer distribution in flow through porous mediums. Water Resources Res. 5:830-839.

Glas, T. K. 1976. The dissolution and transport of gypsum in soils. PhD dissertation, Dept. of Agronomy, Colorado State University, Fort Collins.

Grover, B. L. and Lamborn, R. E. 1970. Preparation of porous ceramic cups to be used for extraction of soil water having low solute concentrations. Soil Sci. Soc. Amer, Proc. 34:707-708.

Gupta, R. K., Millington, R. J. and Klute, A. 1973a. Hydrodynamic dispersion in unsaturated porous media. I. Concentration distribution during dispersion. J. Ind. Soc. Soil Sci. 21:1-7.

Gupta, R. K., Millington, R. J. and Klute, A. 1973b. Hydrodynamic dispersion in unsaturated porous media. II. The stagnant zone concept and the dispersion coefficient. J. Ind. Soc. Soil Sci. 21:121-128.

Levich, V. G.1962. Physicochemical hydrodynamics. Prentice-Hall, Englewood Cliffs, N. J.

Longenecker, D. E. and Lyerly, P. J. 1959. Chemical characteristics of soils of West Texas as affected by irrigation water quality. Soil Sci. 87:207-216.

Massoumi, A. and Cornfield, A. M. 1963. A rapid method for determining sulphate in water extracts of soils. Analyst 88:321-322.

Millington, R. J. and Powrie, J. K. 1968. Dissolution and leaching of fertilizer granules. Trans. 9th int. Congres of Soil Sci. 3:385-391.

Nakayama, F. S. 1971. Problems associated with the determination and application of the solubility product constant. Soil Sci. Soc. Amer. Proc. 35:442-445.

Nernst, W. 1904. Theorie der reaktionsgeschwindigkeit in heterogenen systemen. Z. Phys. Chem. 47:52-55.

Nielsen, D. R. and Biggar, J. W. 1961. Miscible displacement in soils: I. Experimental information. Soil Sci. Soc. Amer. Proc. 25:1-5.

Nielsen, D. R. and Biggar, J. W. 1962. Miscible displacement III. Theoretical considerations. Soil Sci. Soc. Amer. Proc. 26:216-221.

Pfannkuch, H. O. 1962. Contribution a l'étude des déplacements des fluides miscibles dans un milieu poreux. Int. Français du Pétrole.

Powell, M. J. D. 1964. An efficient method for finding the minimum of a function of several variables without calculating derivatives. The Computer J. 7:155-162.

Raats, P. A. C. and Klute, A. 1968. Transport in soils: the balance of mass. Soil Sci. Soc. Amer. Proc. 32:161-166.

Rance, J. M., Davey, B. G. 1968. Determination of the solubility product of soil constituents such as gypsum. Soil Sci. Soc. Amer. Proc. 32:670-672.

Ranz, W. E. and Marshall, W. R. Jr. 1952. Evaporation from drops. Part I. Chem. Eng. Prog. 48:141-146.

Reginato, R. J. and Van Bavel, C. H. M. 1962. Pressure cell for soil cores. Soil Sci. Soc. Amer. Proc. 26:1-3.

Rose, D. A. 1973. Some aspects of the hydrodynamic dispersion of solutes in porous materials. J. Soil Sci. 24:284-295.

Rose, D. A. and Passioura, J. B. 1971a. The analysis of experiments on hydrodynamic dispersion. Soil Sci. 111:252-257.

Shchukarev, A. N. 1891. Reaktionsgeschwindigkeiten zwischen metallen und haloiden. Z. Phys. Chem. 8:76-82.

Smajstrla, A. B., Reddell, D. L. and Hiler, E. A. 1974. Simulation of miscible displacement in soils. Paper presented at the 1974 Annual Meeting Amer. Soc. Agric. Eng., Oklahoma State Univ., Stillwater, Oklahoma.

Smith, S. J. 1972. Relative rate of chloride movement in leaching of surface soils. Soil Sci. 114:259-263.

Swartzendruber, D. and Barber, S. A. 1965. Dissolution of limestone particles in soil. Soil Sci. 100:287-291.

Tanji, K. K. 1969. Solubility of gypsum in aqueous electrolytes as affected by ion association and ionic strength up to 0.15 M and at 25°C. Env. Sci. Techn. 3:656-670.

Tanji, K. K., Doneen, L. D. and Paul, J. L. 1967. Quality of percolating water. III. The quality of waters percolating through stratified substrata, as predicted by computer analysis. Hilgardia 38:319-353.

U. S. Salinity Lab. Staff. 1954. Diagnosis and improvement of saline and alkali soils. USDA. Agr. Handbook No. 60. L. A. Richards (ed).

Weyl, P. 1958. The solution kinetics of calcite. J. Geology 66:163-176.

Williams, D. E. 1948. A rapid manometric method for the determination of carbonate in soils. Soil Sci. Soc. Amer. Proc. 13:127-129.

Wygal, R. J. 1963. Construction of models that simulate oil reservoirs. Soc. Petrol. Eng. J. 3:281-286.

Zangwill, W. I. 1967. Minimizing a function without calculating derivatives. The Computer J. 10:293-296.